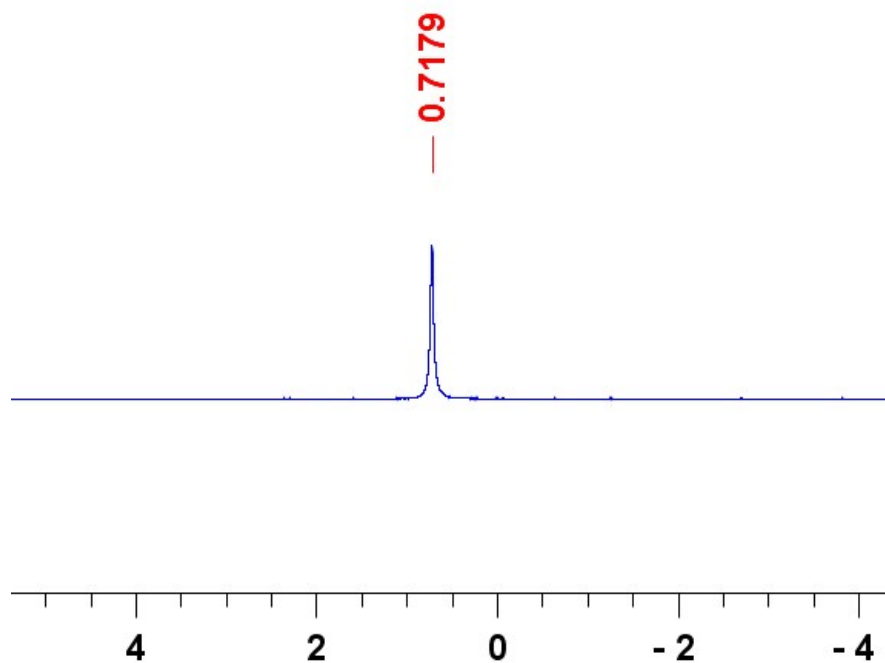


## Electronic Supplementary Information

### Modifying the Donor Properties of *Tris*(pyridyl)aluminates in Lanthanide (II) Sandwich Compounds

Raúl García-Rodríguez,<sup>a\*</sup> Sara Kopf,<sup>b</sup> and Dominic S. Wright<sup>b</sup>

## $^7\text{Li}$ NMR spectrum of LiI-containing $[\text{EtAl}(\text{6-Me-2-py})_3]_2\text{Yb}$ ( $\mathbf{4}\cdot\text{LiI}$ )



**Figure S1**  $^7\text{Li}$  NMR spectrum (+25 °C, 194 MHz, thf - $d_8$ ) of  $\mathbf{4}\cdot\text{LiI}$ . The spectroscopic properties for the  $[\text{EtAl}(\text{6-Me-2-py})_3]_2\text{Yb}$  complex in  $\mathbf{4}\cdot\text{LiI}$  are identical to those observed for **4** (see NMR spectra for compound **4**, Fig S12) with the exception of the presence of  $\text{LiI}(\text{thf})_3$  in the  $^7\text{Li}$  NMR (+25 °C,  $d_8$ -THF, 194 MHz),  $\delta = 0.72$  (s) ppm and the presence of thf in the  $^1\text{H}$  NMR (+25 °C,  $d_8$ -thf, 400 MHz),  $\delta = 3.62$  (m,  $-\text{CH}_2-\text{O}$ , thf), 2.77 1.77 (m,  $-\text{CH}_2-$ , thf).

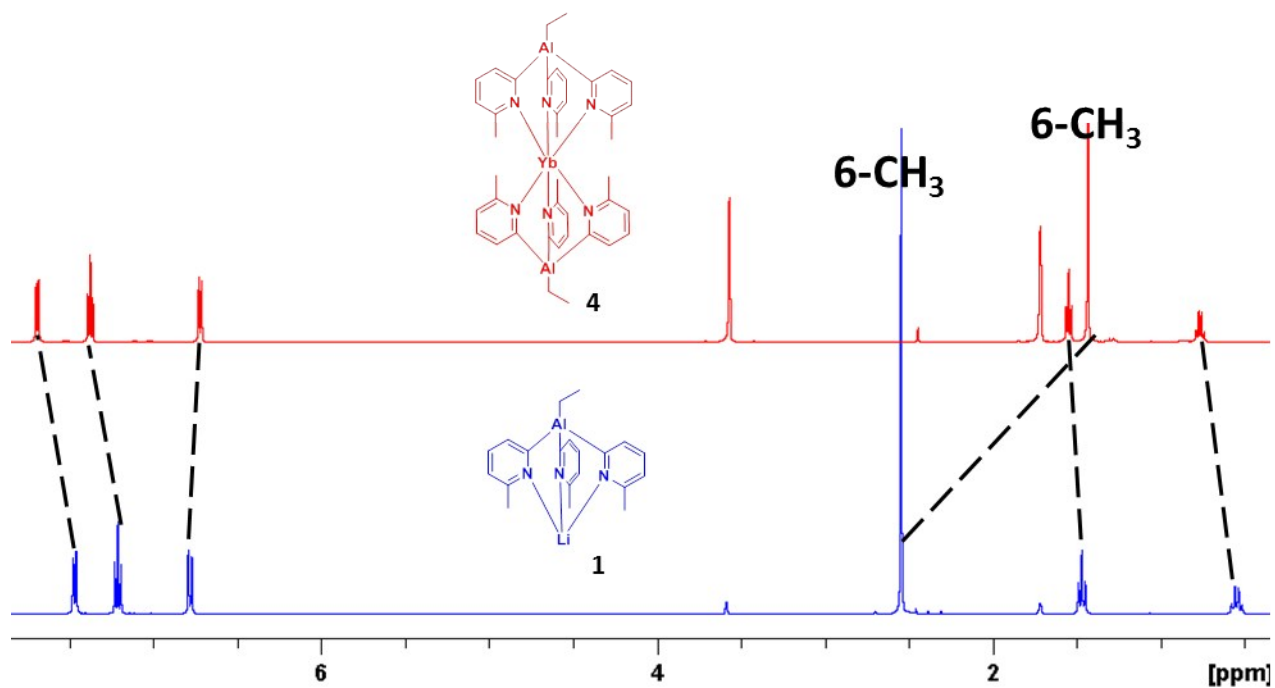


**Figure S2** Stacked  $^1\text{H}$  NMR spectra (+25 °C, 500 MHz,  $\text{thf-d}_8$ ) comparing the differences in the chemical shift of the signals of compound **4** and its starting material (**1**). Coordination to  $\text{Yb}^{2+}$  results in a significant upfield shift of the 6-Me group by 1.1 ppm.

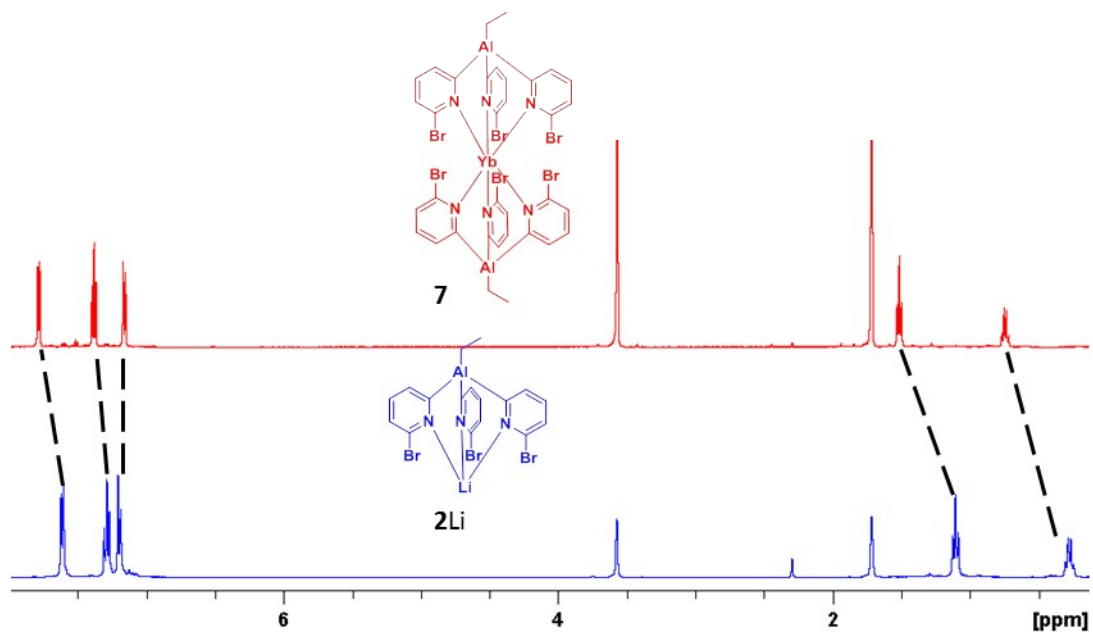


**Figure S3** Stacked <sup>1</sup>H NMR spectra (+25 °C, 500 MHz, thf-d<sub>8</sub>) comparing the differences in the chemical shifts of the signals of compound **7** and its starting material (**2Li**).

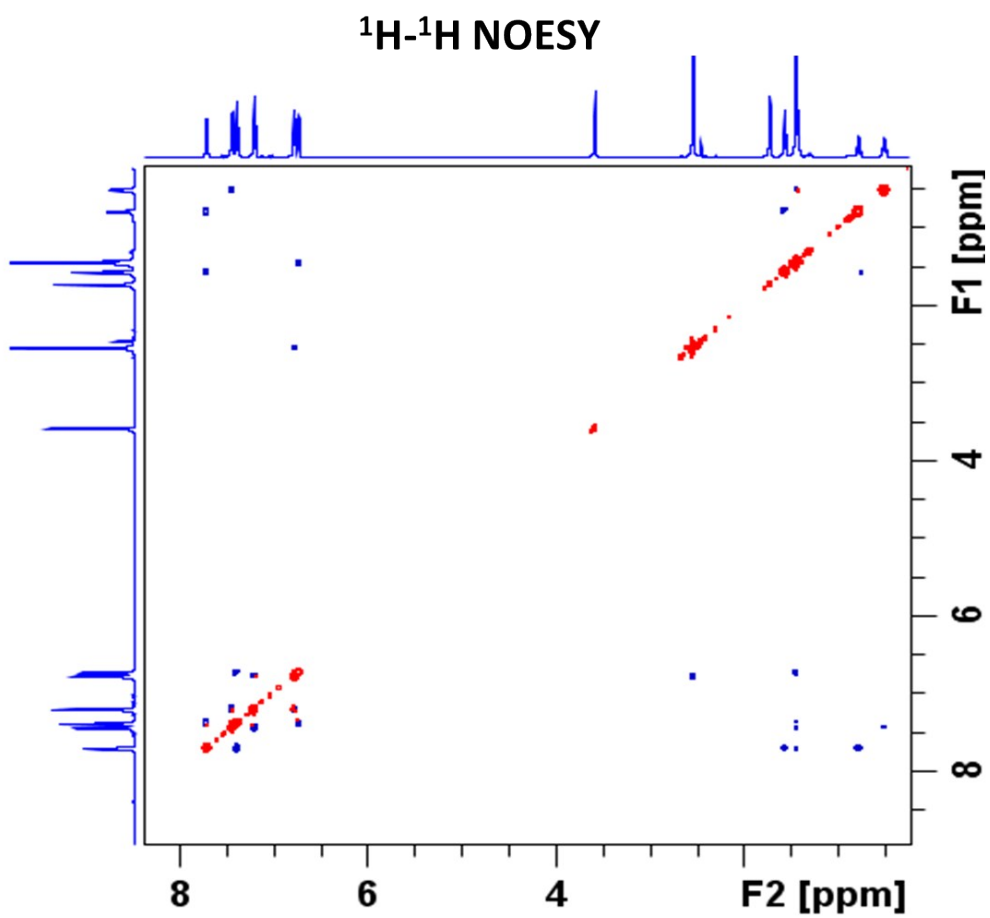


**Figure S4**  $^1\text{H}$ - $^1\text{H}$  NOESY spectrum of a mixture of **1Li** and **4** in  $\text{thf-d}_8$ . No chemical exchange was observed. See also Fig S5.

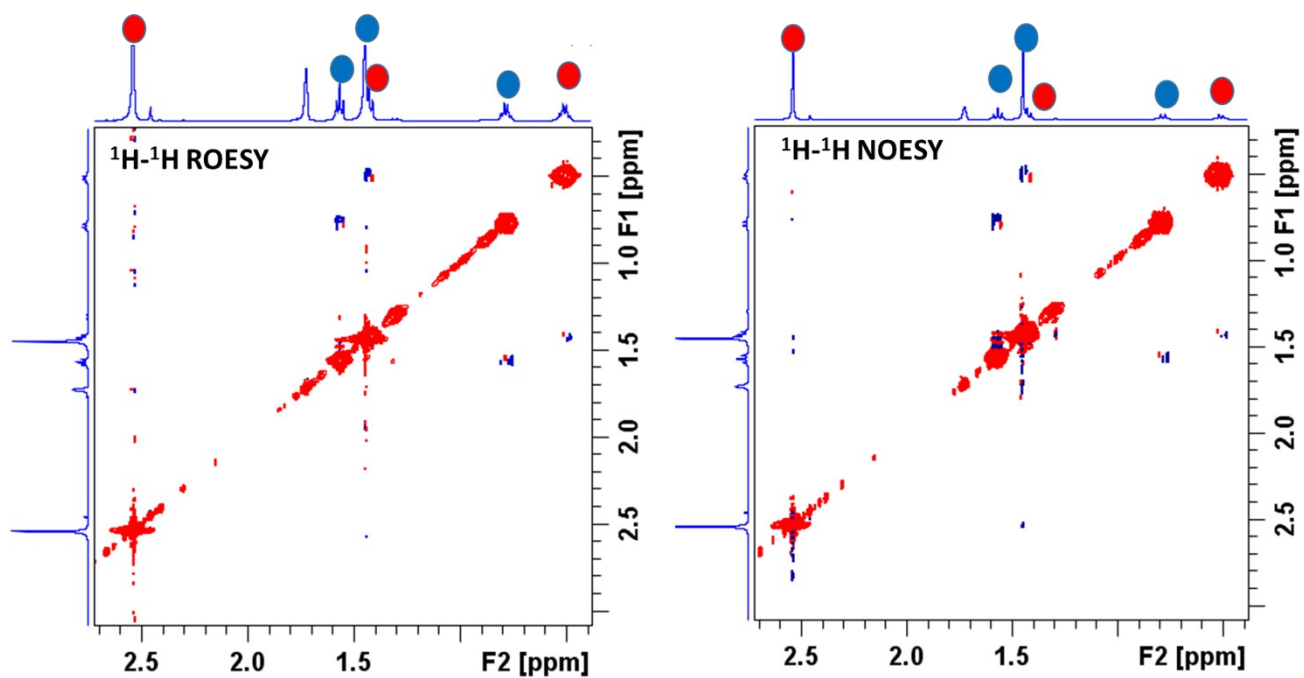


**Figure S5**  $^1\text{H}$ - $^1\text{H}$  ROESY (ethyl region, left) and  $^1\text{H}$ - $^1\text{H}$  NOESY (ethyl region, right) spectra of a mixture of 1Li and 4 in  $\text{thf-d}_8$ . Colour code: 4 (blue circles), 1Li (red circles). No chemical exchange was observed.

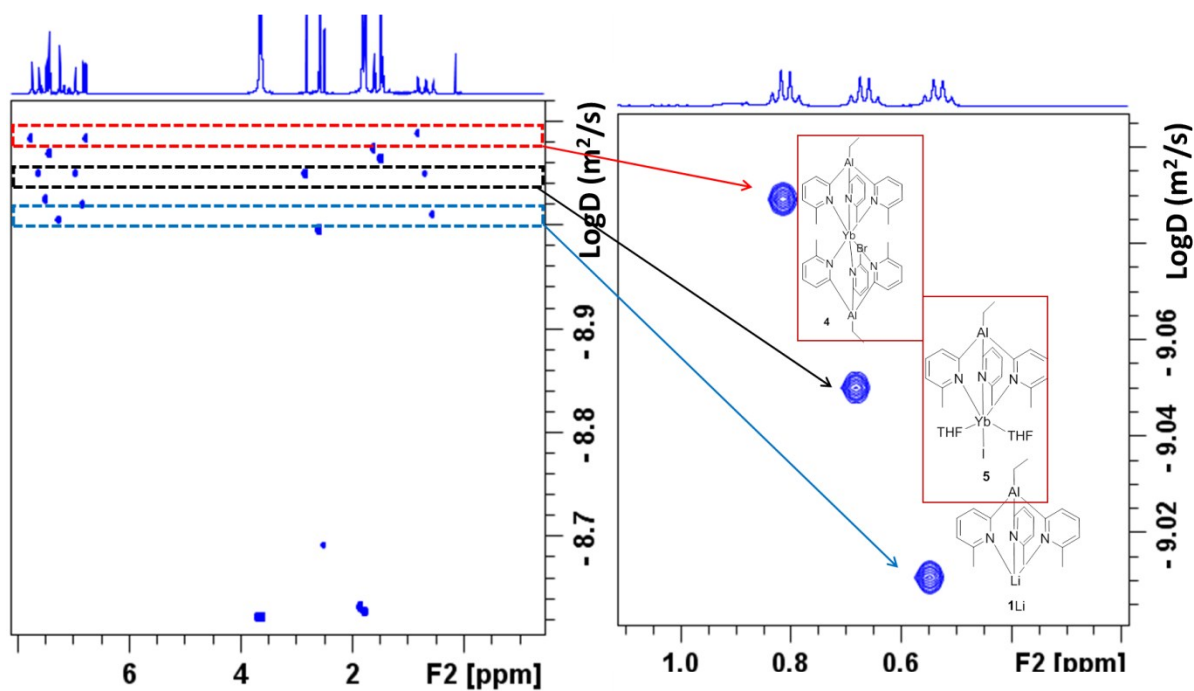


**Figure S6**  $^1\text{H}$  DOSY spectrum of a mixture of aluminate **1Li**, sandwich compound **4** and the half-sandwich **5** in  $\text{THF-d}_8$  at  $25\text{ }^\circ\text{C}$ . Although several signals overlapped, the  $\text{CH}_2$  groups of the three species appear in well separated regions (left). The diffusion coefficients of the three species follow the expected trend based on their hydrodynamic radii, which in turns reflects their relative sizes: **4**>**5**>**1Li**.

Note: A small amount of free 2-methylpyridine was also present ( $\text{CH}_3$  group clearly observed at  $2.46(\text{s})$ ).

Note 2: Dashed boxes and colours are guides to the eye.

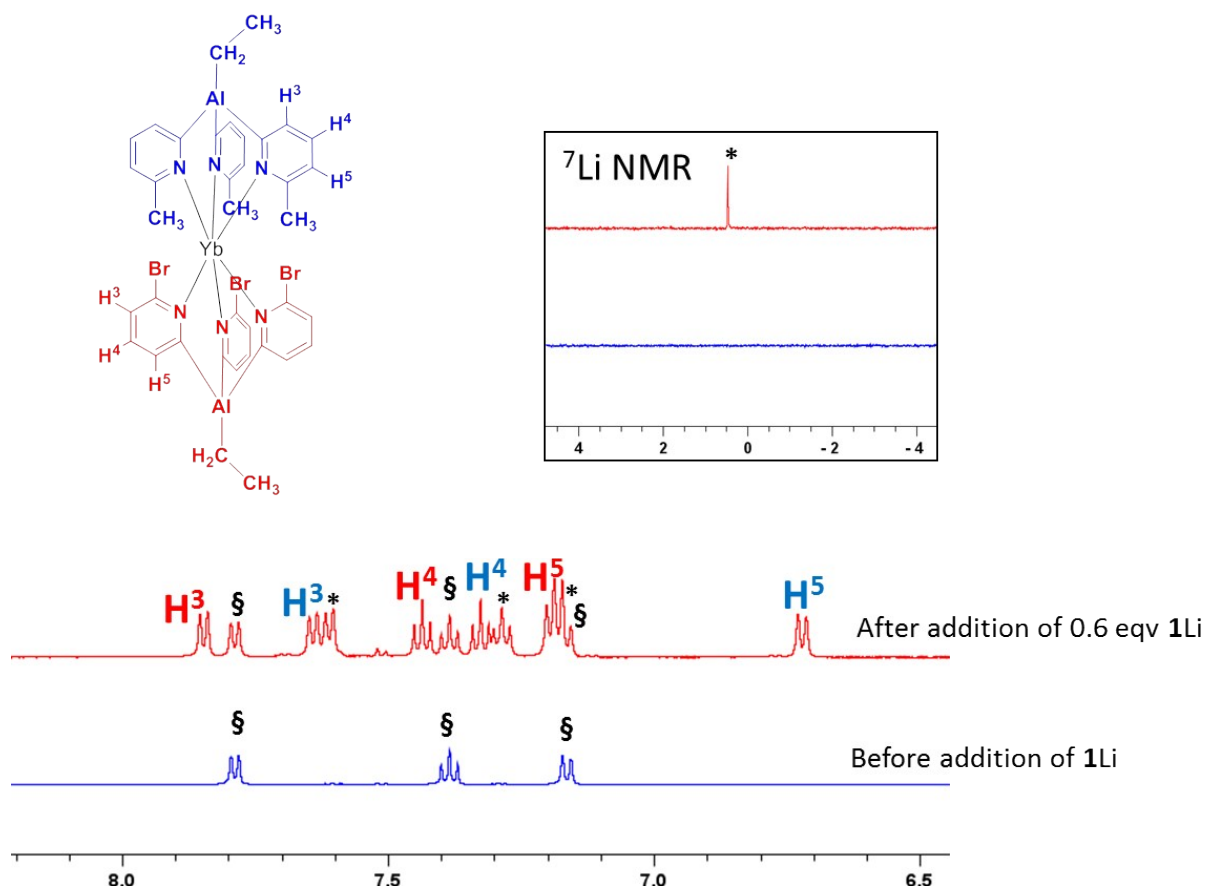


**Figure S7.**  $^1\text{H}$  NMR (+25 °C,  $\text{thf-d}_8$ , 500 MHz) and  $^7\text{Li}$  NMR (+25 °C, 194 MHz,  $\text{THF-d}_8$ ) spectra (insert) of a solution of sandwich ytterbium complex  $[\text{EtAl}(6\text{-Br-2-py})_3]_2\text{Yb}$  (**7**) (labelled as § in the spectra) in  $\text{thf-d}_8$  before (blue spectrum) and 30 min after (red spectrum) the addition of 0.6 eqv of **1Li** (red spectrum). The reaction results in the formation of the heteroleptic Yb(II) sandwich compound  $[\{\text{EtAl}(6\text{-Me-2-py})_3\}\{\text{EtAl}(6\text{-Br-2-py})_3\}\text{Yb}]$  (**9**) and the formation of **2Li** (labelled as \* in the spectra) in a 1:1 ratio. The assignments of the signals for the heteroleptic Yb(II) sandwich compound (**9**) which contains the 6-Me ligand **1** (blue) and the 6-Br ligand **2** (red) are labelled in the  $^1\text{H}$  NMR spectrum following the atom labels shown in the figure. Subsequent addition of further equivalents of **1Li** results in the complete disappearance of **7**, and eventually of **9**, along with the formation of  $[\text{EtAl}(6\text{-Me-2-py})_3]_2\text{Yb}$  (**4**) and **2Li** (\*), see Figure S8.

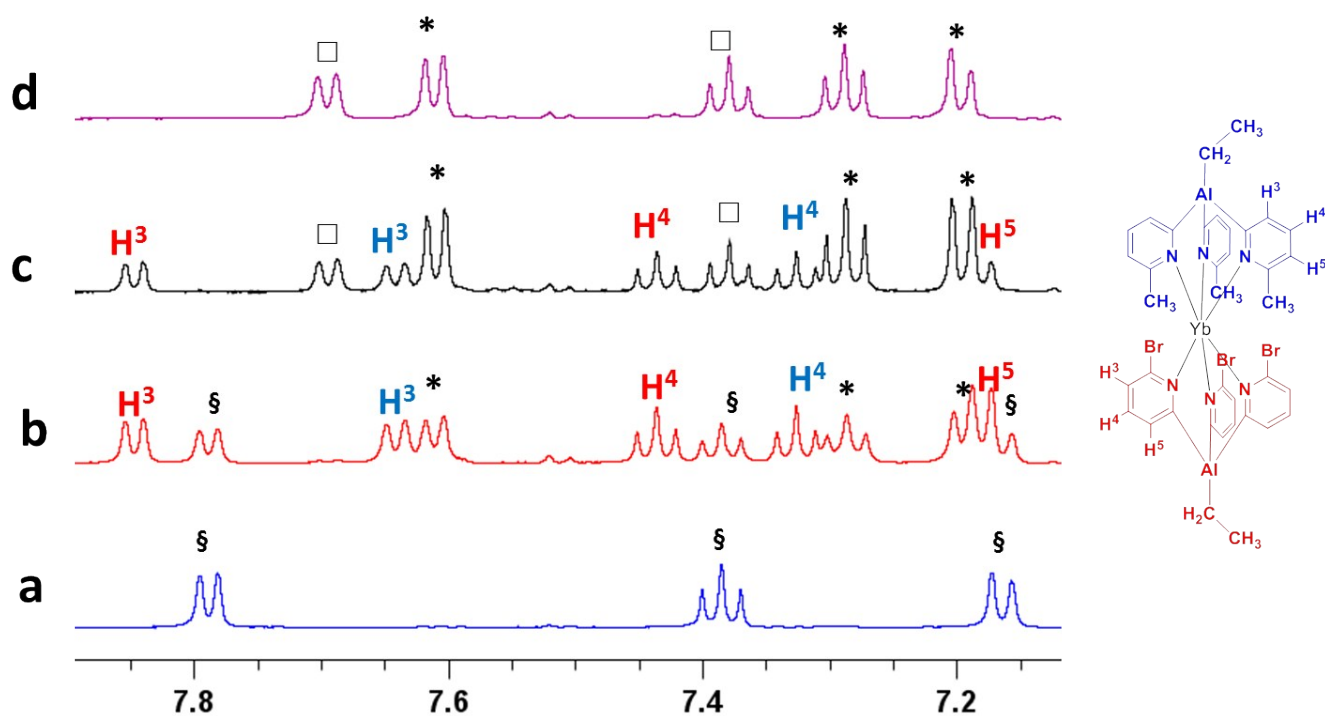


**Figure S8** Stacked  $^1\text{H}$  NMR (+25  $^\circ\text{C}$ ,  $\text{thf-d}_8$ , 500 MHz) spectra of a solution of the ytterbium sandwich complex  $[\text{EtAl}(\text{6-Br-2-py})_3]_2\text{Yb}$  (**7**) (labelled as  $\S$  in the spectra): a) before the addition of **1Li**; b) after the addition of 0.6 eqv of **1Li**; c) after the addition of *ca* 1.5 eqv of **1Li**; and d) after the addition of *ca* 2 eqv of **1Li**. The reaction involves the initial formation of the heteroleptic Yb(II) sandwich compound  $[\{\text{EtAl}(\text{6-Me-2-py})_3\}\{\text{EtAl}(\text{6-Br-2-py})_3\}\text{Yb}]$  (**9**) and the formation of **2Li** (labelled as \* in the spectra). Further addition of **1Li** results in the complete disappearance of **7**, and eventually of **9**, along with the formation of  $[\text{EtAl}(\text{6-Me-2-py})_3]_2\text{Yb}$  (**4**) (labelled as  $\square$  in the spectra) and **2Li** (\*).

Note: All the spectra were taken after allowing enough reaction time to ensure that all  $[\text{EtAl}(\text{6-Me-2-py})_3]\text{Li}$  (**1Li**) could react completely.

Reaction key:  $[\text{EtAl}(\text{6-Br-2-py})_3]_2\text{Yb}$  (**7**) =  $\S$ ;  $[\text{EtAl}(\text{6-Br-2-py})_3]\text{Li}$  (**2Li**) = \*;  $[\text{EtAl}(\text{6-Me-2-py})_3]_2\text{Yb}$  (**4**) =  $\square$ . The assignment of the signals of the heteroleptic Yb(II) sandwich compound  $[\{\text{EtAl}(\text{6-Me-2-py})_3\}\{\text{EtAl}(\text{6-Br-2-py})_3\}\text{Yb}]$  (**9**) which contains the 6-Me ligand **1** (blue) and the 6-Br ligand **2** (red) are labelled in the  $^1\text{H}$  NMR spectrum following the atom labels shown in the figure.

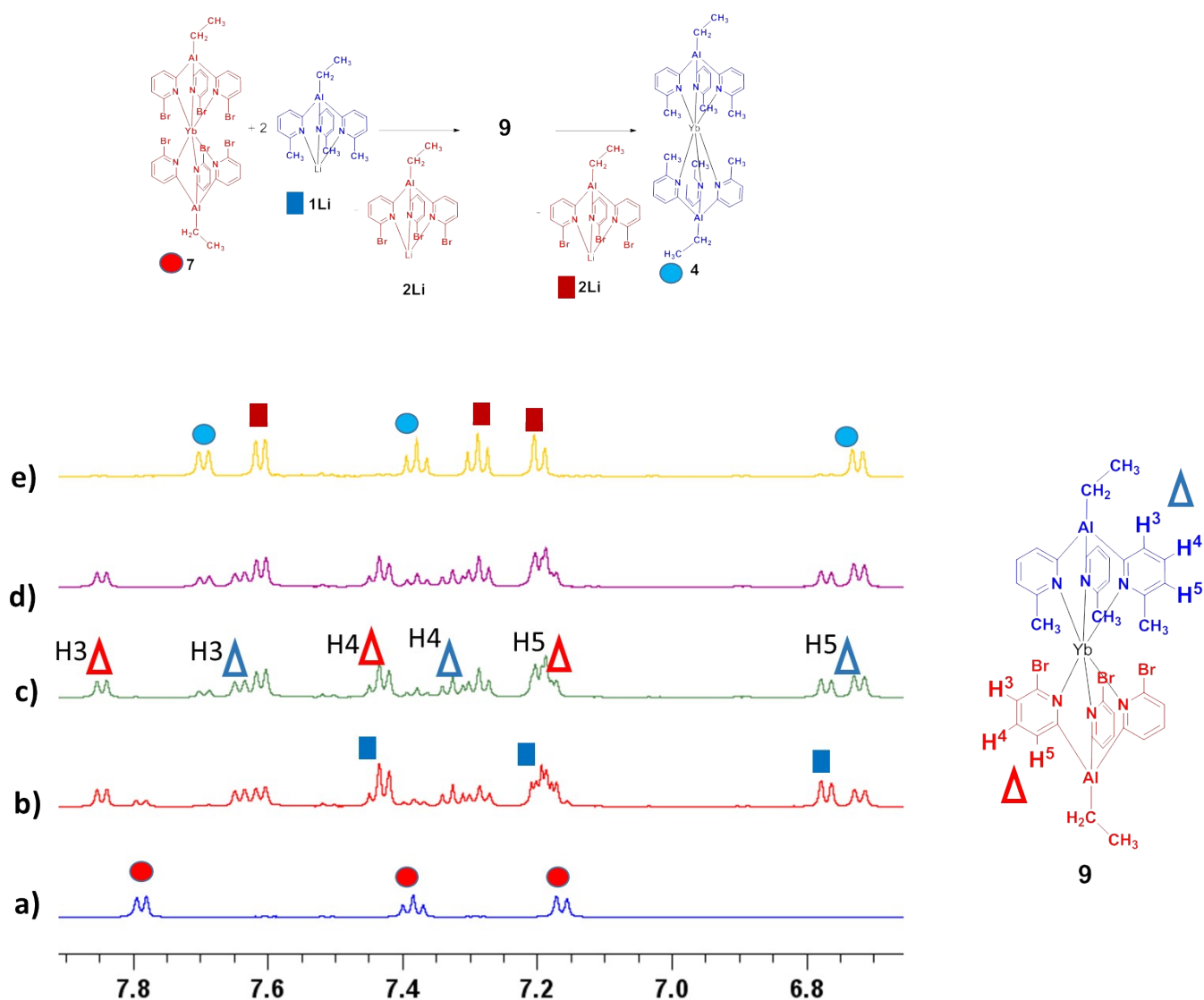


**Figure S9** Stacked  $^1\text{H}$  NMR spectra (+25°C, 500 MHz,  $\text{THF-d}_3$ ) of the time evolution of the reaction of *ca* 2 equivalents of **1Li** with **7** in thf at room temperature to give  $[\text{EtAl}(\text{6-Me-2-py})_3]_2\text{Yb}$  (**4**) and **2Li**. The reaction involves the heteroleptic Yb(II) sandwich compound  $[\{\text{EtAl}(\text{6-Me-2-py})_3\}\{\text{EtAl}(\text{6-Br-2-py})_3\}\text{Yb}]$  (**9**) as an intermediate. a) Yb(II) sandwich **7** before the addition of **1Li**; b) 15 min after the addition of **1Li**, most of **7** is consumed and there is still unreacted **1Li**. The  $^1\text{H}$  NMR spectrum shows the formation of intermediate **7** along with concomitant formation of **2Li**. c) After 1 h, no appreciable amounts of the ytterbium sandwich complex **7** are observed, while the amount of **2Li** has increased and a small amount of homoleptic complex **4** is observed in addition to **9**. The signals of the heteroleptic Yb(II) sandwich compound  $[\{\text{EtAl}(\text{6-Me-2-py})_3\}\{\text{EtAl}(\text{6-Br-2-py})_3\}\text{Yb}]$  (**9**) which contains the 6-Me ligand **1** (blue triangles) and the 6-Br ligand **2** (red triangles) are labelled in the  $^1\text{H}$  NMR spectrum. The two spin systems were assigned with the help of a  $^1\text{H}$ - $^1\text{H}$  COSY experiment. The H<sub>3</sub> and H<sub>4</sub> pyridyl signals for both ligands in **7** are clearly resolved. However, while the H<sub>3</sub> and H<sub>4</sub> pyridyl signals do not overlap with their corresponding Li salts and/or Yb homoleptic sandwich complexes, the H<sub>5</sub> protons of **9** overlap with the H<sub>5</sub> protons of **4** and **2Li** respectively. d) After 150 min the amount of heteroleptic complex **9** decreases, and the concomitant formation of homoleptic complexes **4** and **2Li** is observed. e) After 36 h no heteroleptic complex **9** is observed and only homoleptic complex **4** and **2Li** are observed. See also Figures S10 and S11

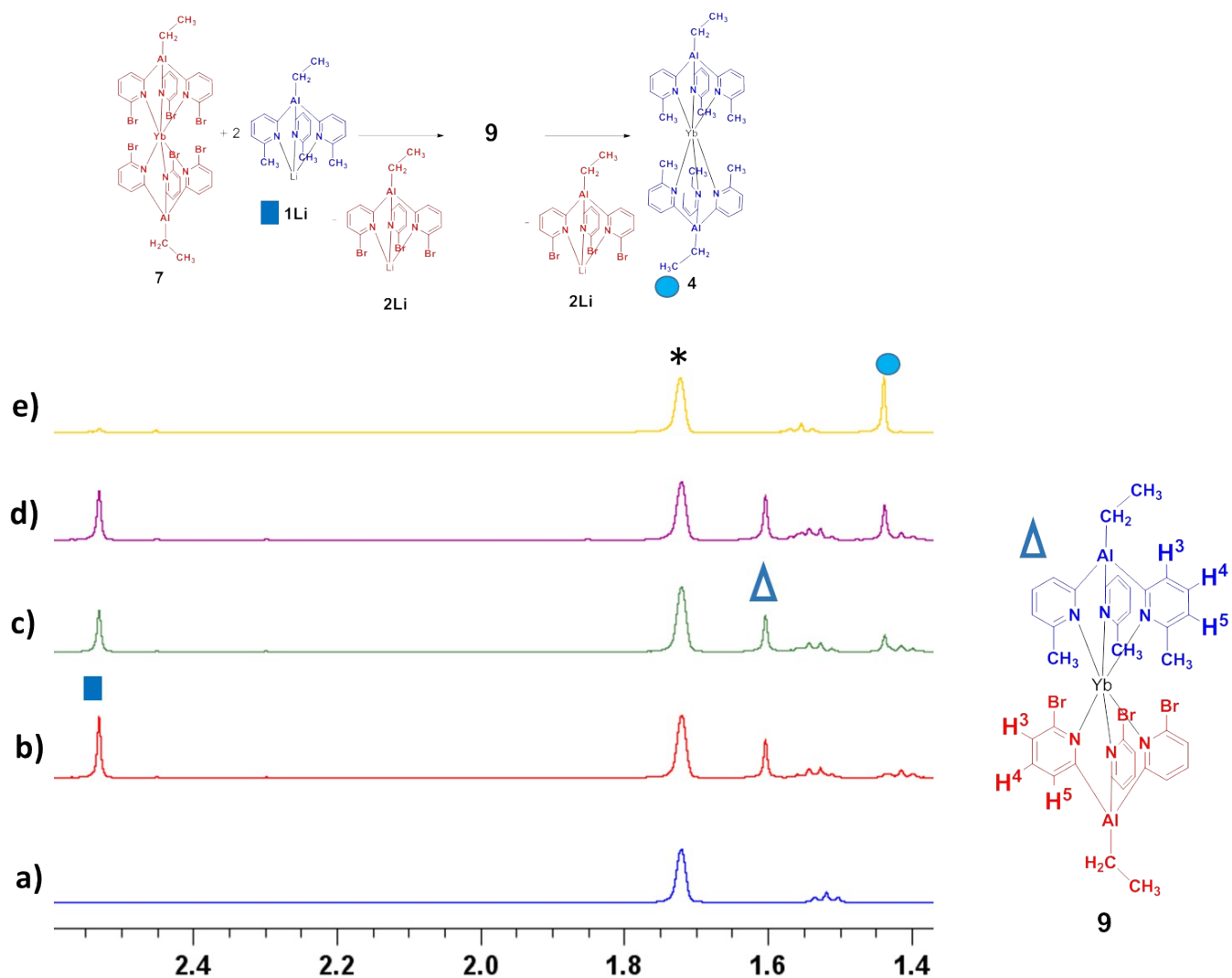
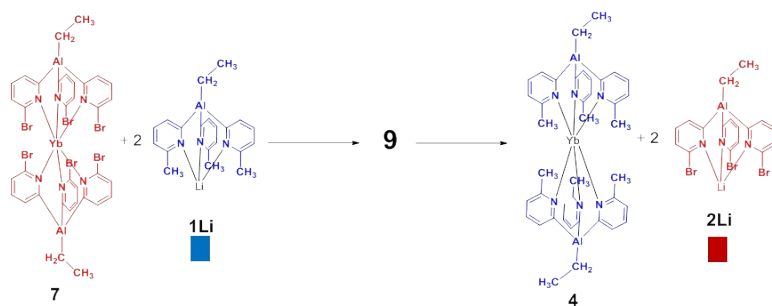


**Figure S10** Stacked  $^1\text{H}$  NMR spectra of the 6-Me-Py region (+25°C, 500 MHz, THF- $d_8$ ) during the time evolution of the reaction of *ca* 2 equivalents of **1Li** with **7** in thf at room temperature to give  $[\text{EtAl}(6\text{-Me-2-py})_3]_2\text{Yb}$  (**4**) and **2Li**. (see also Fig S12 for details). The 6-Me-Py region is particularly diagnostic since the greatest change in chemical shift among all the 6-Me ligand **1** signals is found for the 6-Me group:  $\delta = 2.53$  for **1Li** (square),  $\delta = 1.60$  for intermediate heteroleptic complex **9** (triangle) and  $\delta = 1.44$  for **4** (circle).



## $^7\text{Li}$ NMR

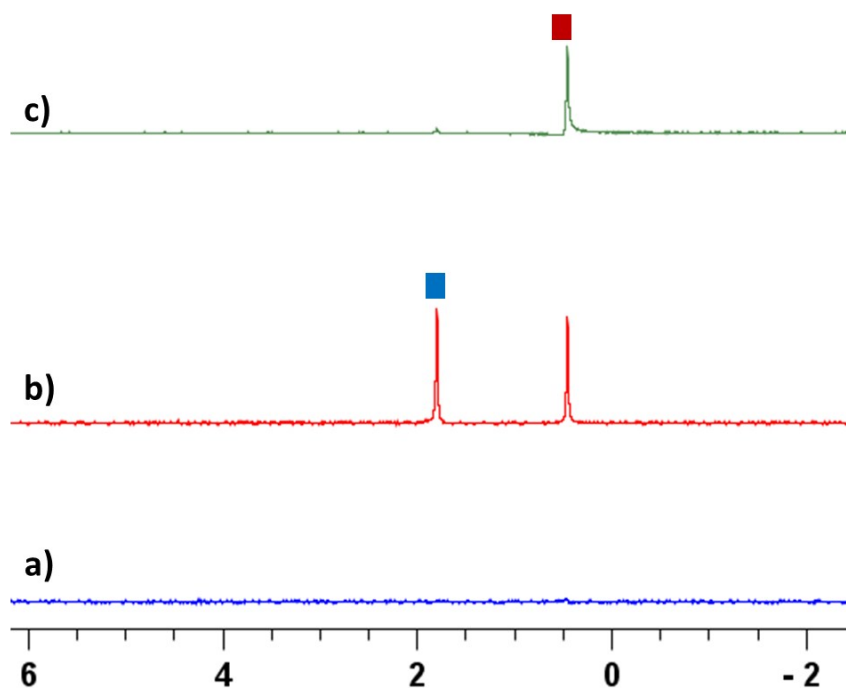


**Figure S11** Stacked  $^7\text{Li}$  NMR spectra (+25°C, 500 MHz, THF- $d_8$ ) during the time evolution of the reaction of *ca* 2 equivalents of **1Li** with **7** in thf at room temperature to give  $[\text{EtAl}(\text{6-Me-2-py})_3]_2\text{Yb}$  (**4**) and **2Li**: a) before the addition of **1Li**, b) after *ca* 30 min and c) after 36 h.

# NMR spectra for compound 4, [EtAl(6-Me-2-py)<sub>3</sub>]<sub>2</sub>Yb

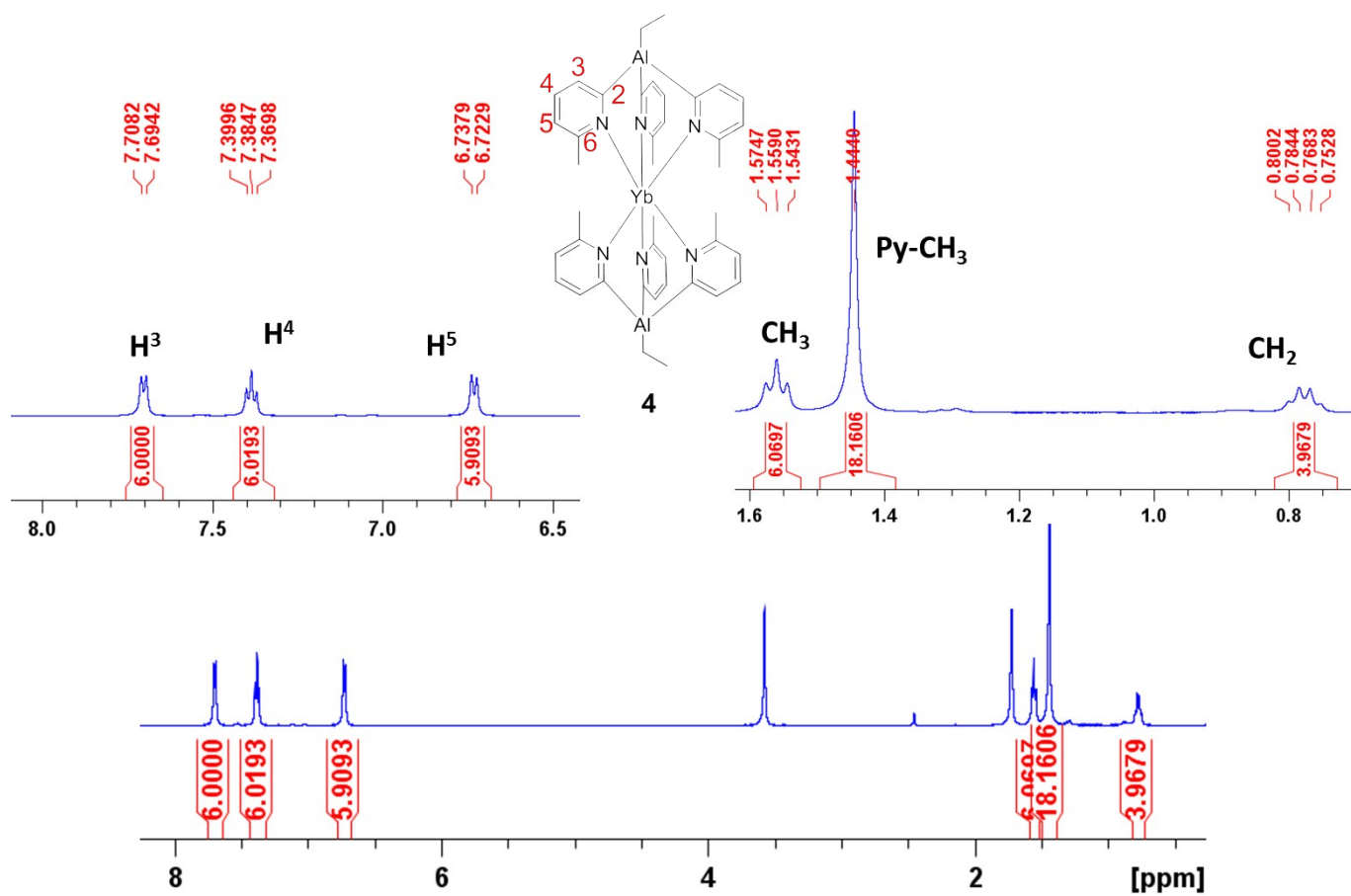


Figure S12 <sup>1</sup>H NMR spectrum (+25 °C, 500 MHz, THF-d<sub>8</sub>) of [EtAl(6-Me-2-py)<sub>3</sub>]<sub>2</sub>Yb (4).

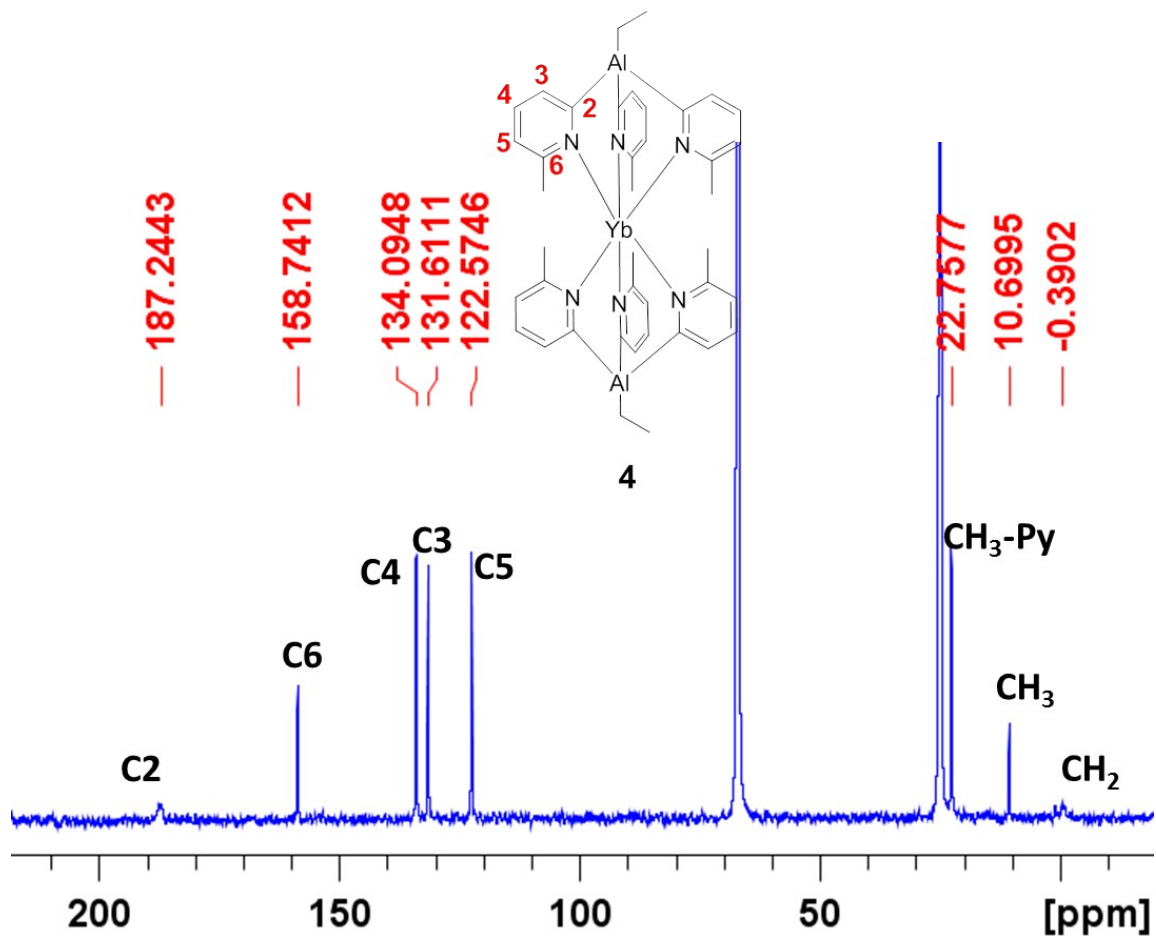
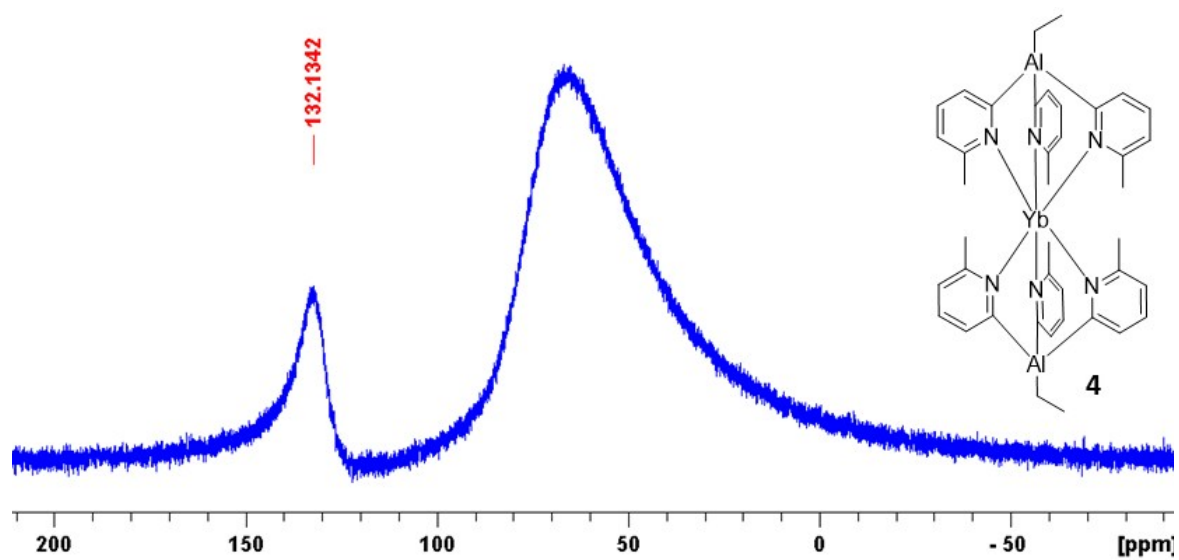
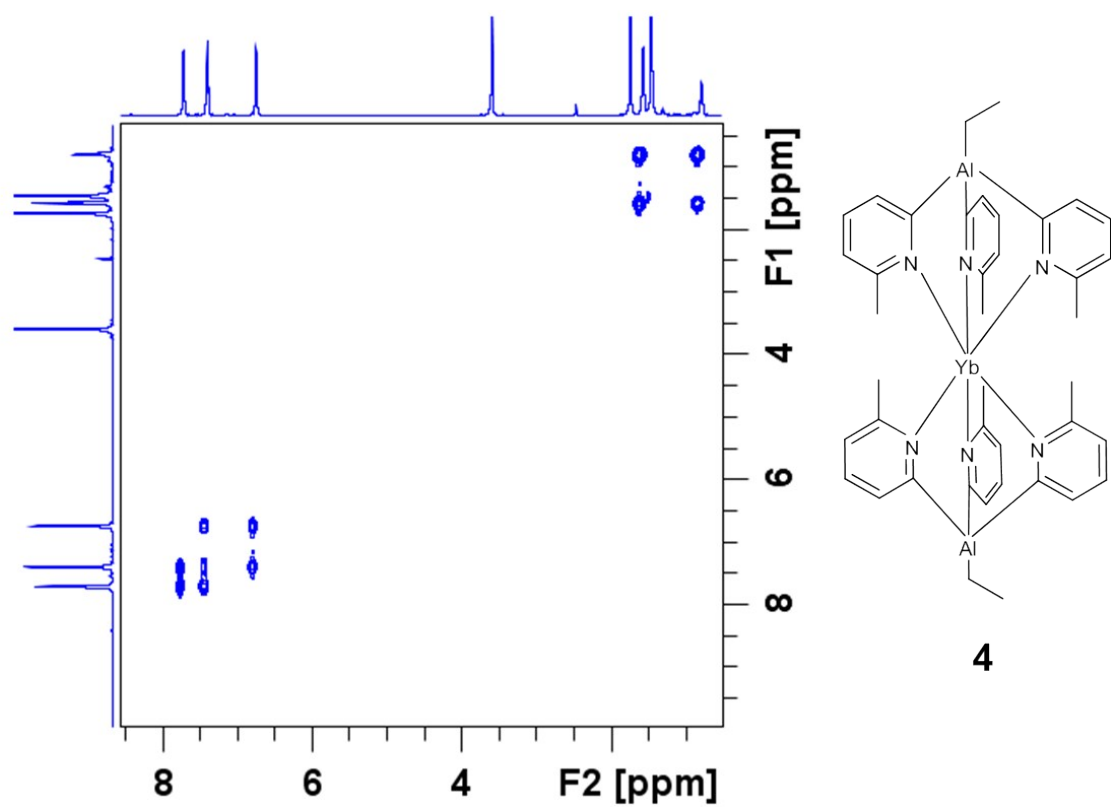


Figure S13  $^{13}\text{C}\{^1\text{H}\}$  NMR spectrum (+25 °C, 126 MHz, THF- $d_8$ ) of  $[\text{EtAl}(\text{6-Me-2-py})_3]_2\text{Yb}$  (4).



**Figure S14**  $^{27}\text{Al}$  NMR spectrum (+25 °C, 130 MHz,  $\text{THF-d}_8$ ) of  $[\text{EtAl}(6\text{-Me-}2\text{-py})_3]_2\text{Yb}$  (**4**).

Note: The broad signal at around 65ppm in the  $^{27}\text{Al}$  NMR spectrum arises from the probe background.



**Figure S15**  $^1\text{H}$ - $^1\text{H}$  COESY NMR spectrum (+25 °C, 500 MHz,  $\text{THF-d}_8$ ) of  $[\text{EtAl}(\text{6-Me-2-py})_3]_2\text{Yb}$  (**4**).

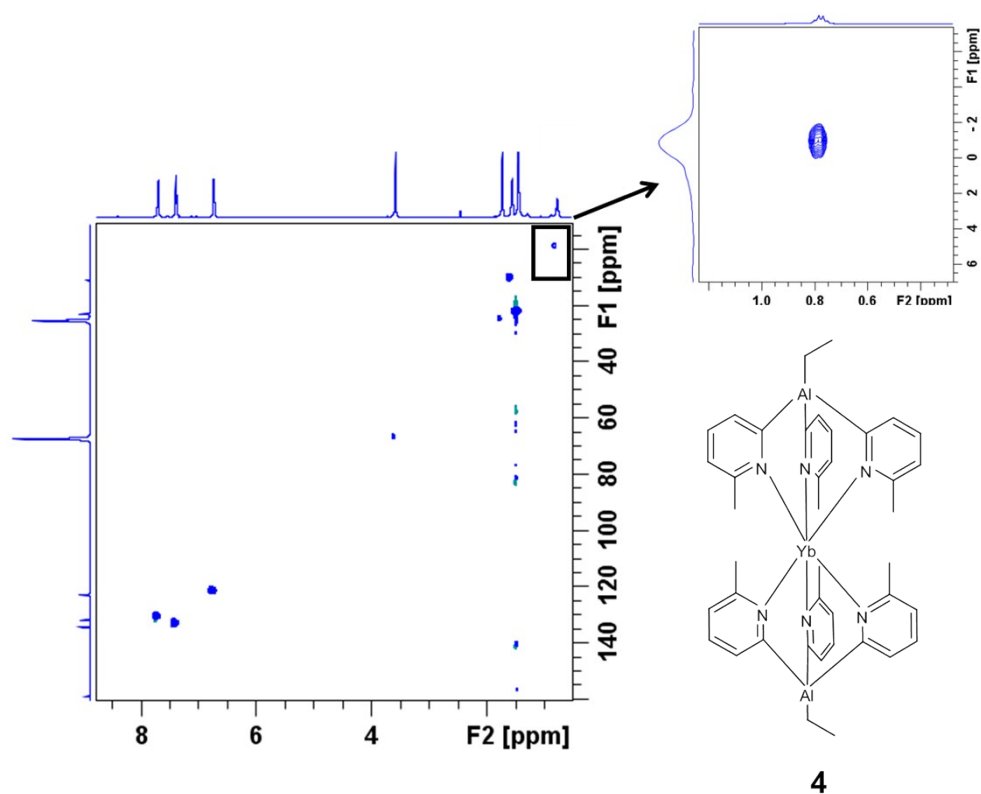


**Figure S16**  $^1\text{H}$ - $^{13}\text{C}$  HMQC NMR spectra (+25 °C, 500 MHz, THF- $d_8$ ) of  $[\text{EtAl}(\text{6-Me-2-py})_3]_2\text{Yb}$  (**4**). Direct observation of the Al-bonded C atoms was difficult in the  $^{13}\text{C}\{^1\text{H}\}$  spectrum due to their low-intensity broad resonances. However, a broad Al-CH<sub>2</sub> signal can be easily detected in the  $^1\text{H}$ - $^{13}\text{C}$  HMQC NMR spectrum (insert).

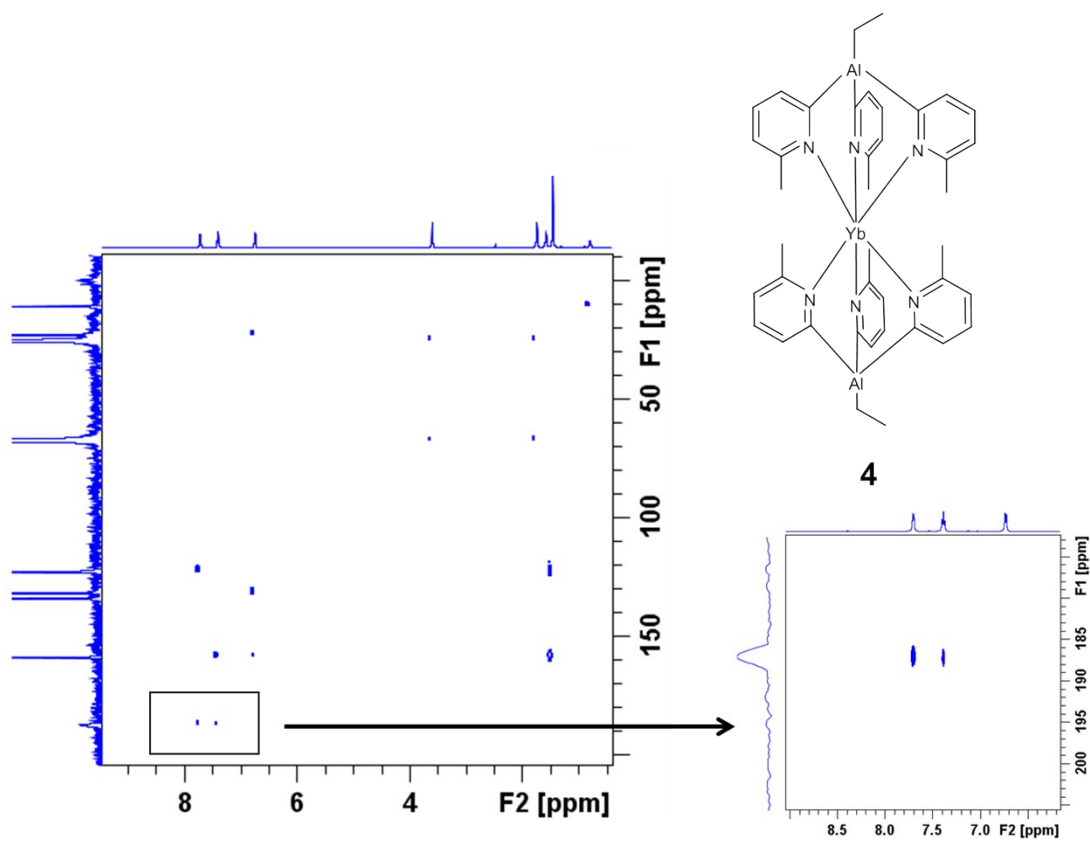


**Figure S17**  $^1\text{H}$ - $^{13}\text{C}$  HMBC NMR spectra (+25 °C, 500 MHz,  $\text{THF-d}_8$ ) of  $[\text{EtAl}(\text{6-Me-2-py})_3]_2\text{Yb}$  (**4**). Direct observation of Al-bonded C atoms was challenging in the  $^{13}\text{C}\{^1\text{H}\}$  spectrum due to their low-intensity broad resonances. However, a broad Al-C(2) signal can be easily detected in the  $^1\text{H}$ - $^{13}\text{C}$  HMBC NMR spectrum (insert).

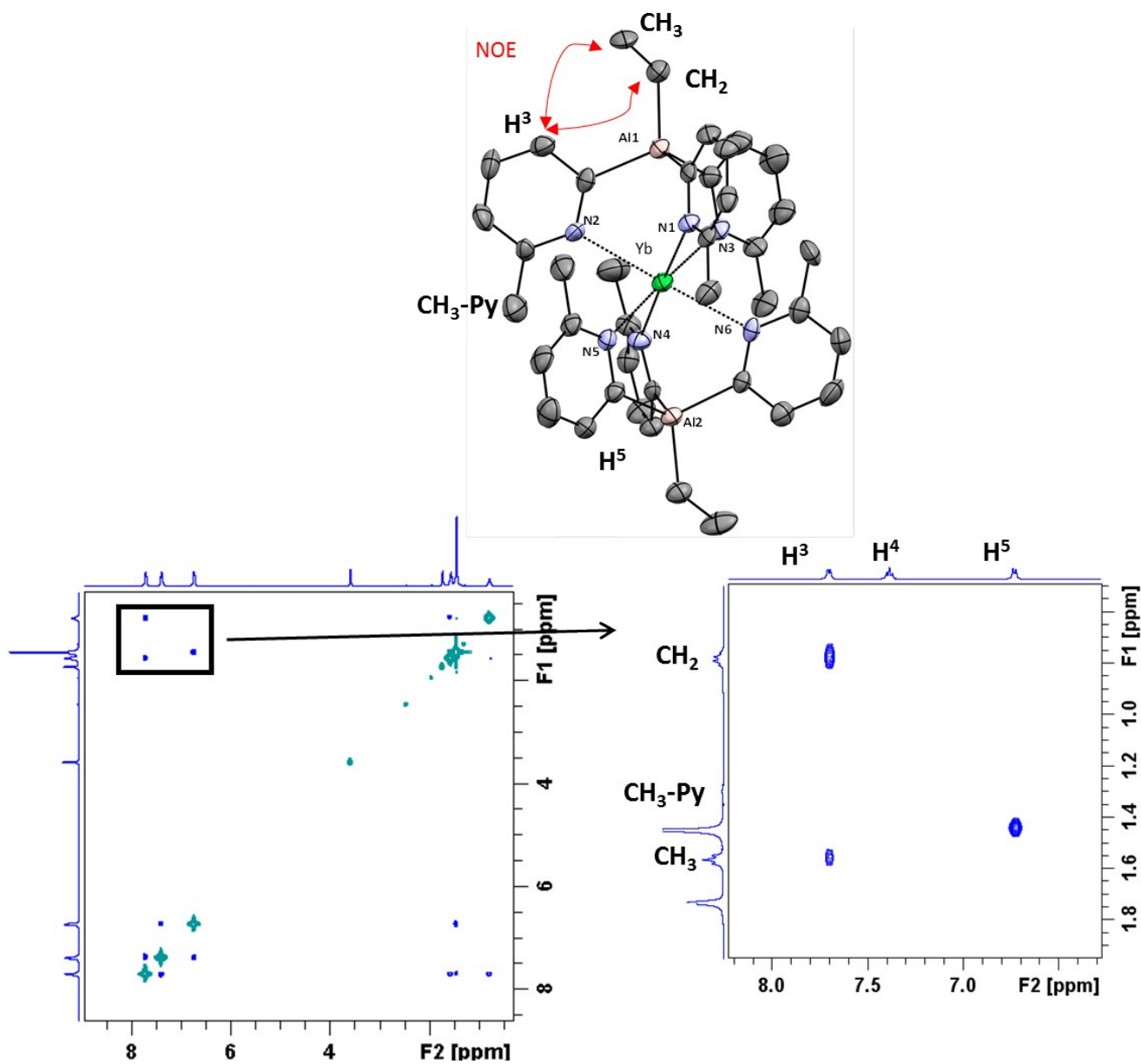


**Figure S18**  $^1\text{H}$ - $^1\text{H}$  NOESY NMR spectrum (+25 °C, 500 MHz, THF- $d_8$ ) of  $[\text{EtAl}(\text{6-Me-2-py})_3]_2\text{Yb}$  (**4**). Crosspeaks observed between the C(3)-H py proton and the Al-CH<sub>2</sub>CH<sub>3</sub> protons, and between the Py-CH<sub>3</sub> protons and aromatic pyridyl protons (C(5)-H) arise from intramolecular cross-relaxation of protons that are close to each other in space, confirming the presence of an Et-Al-Py linkage.

# NMR spectra for compound 5, [EtAl(6-Me-2py)<sub>3</sub>YbI(thf)<sub>2</sub>]

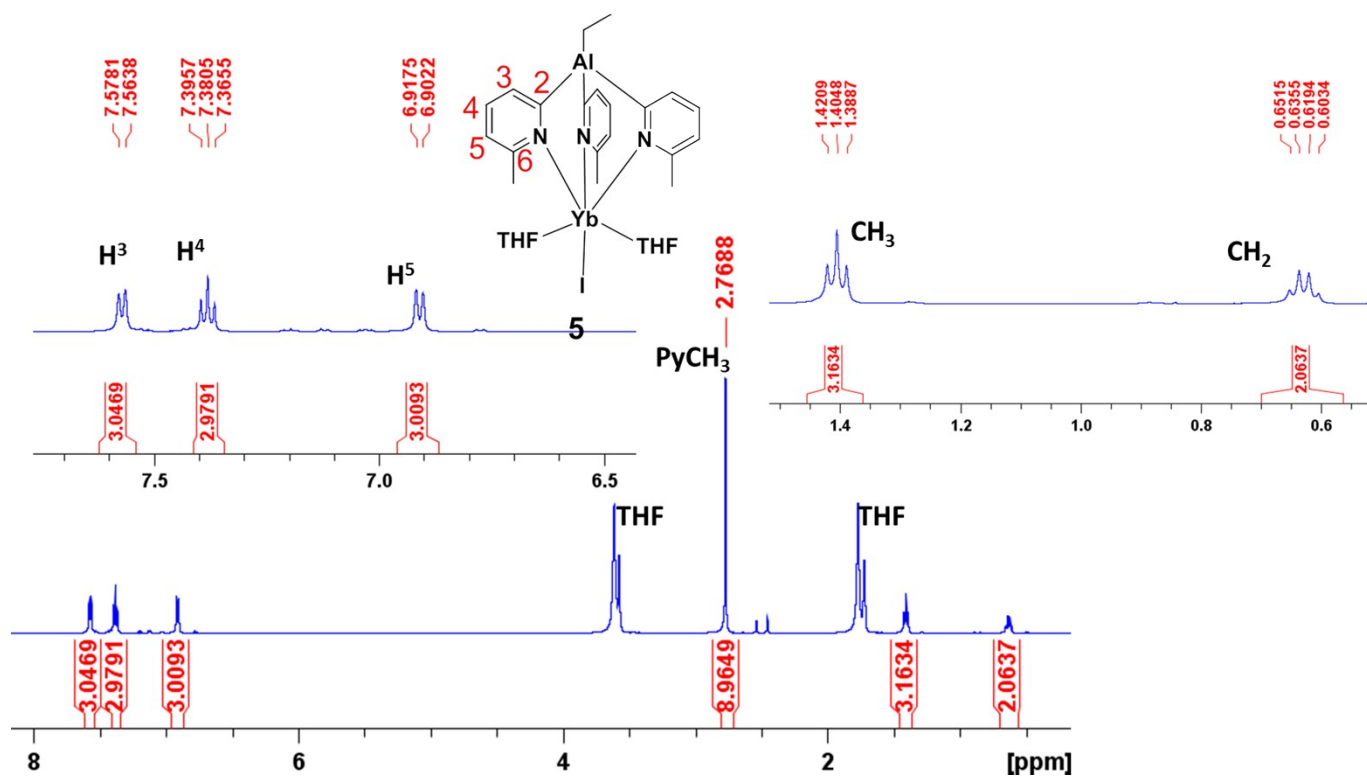
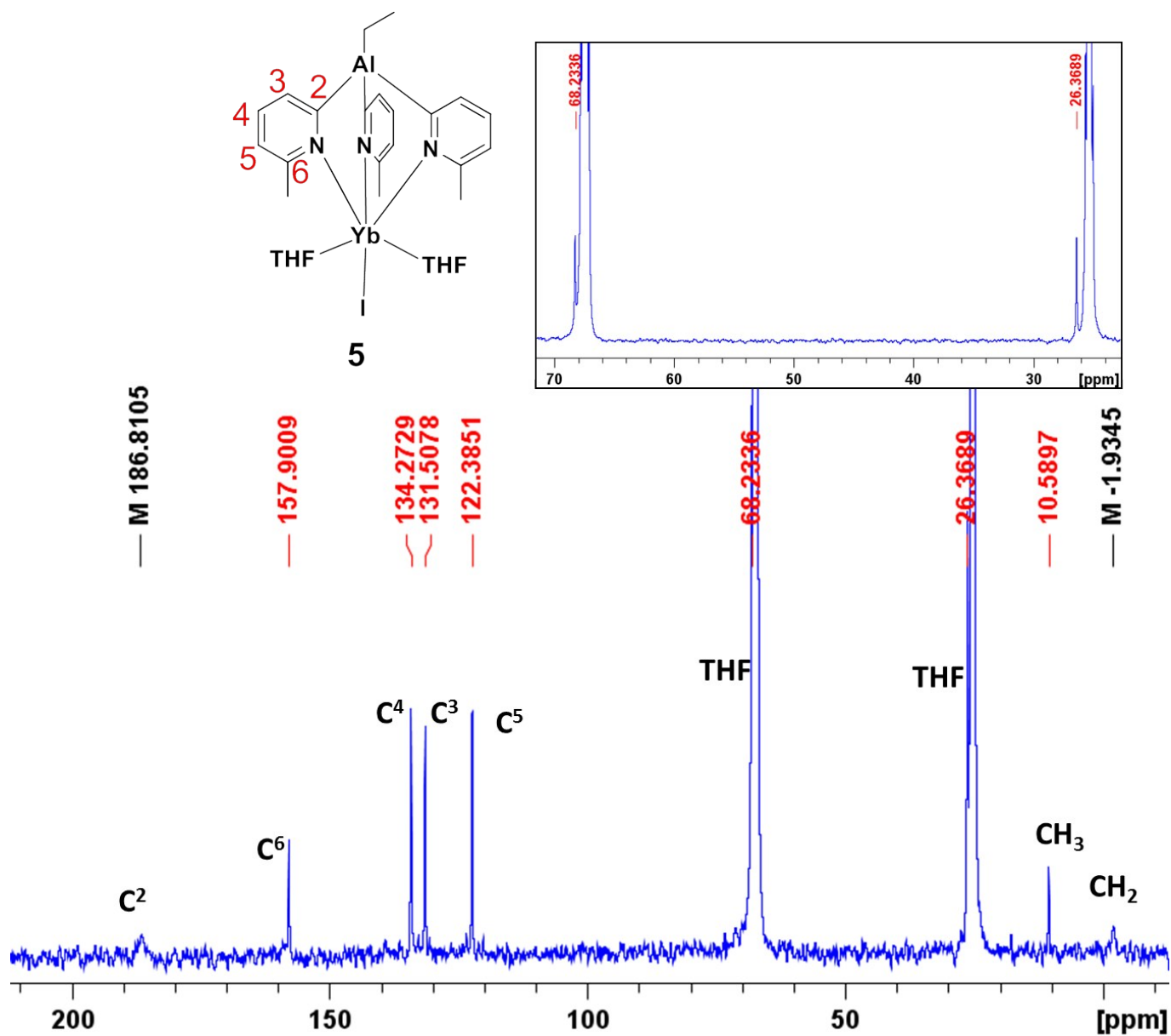


Figure S19 <sup>1</sup>H NMR spectrum (+25 °C, 126 MHz, THF-d<sub>8</sub>) of [EtAl(6-Me-2py)<sub>3</sub>YbI(thf)<sub>2</sub>] (5). The signals of THF appear partially overlapped with the signals of THF-d<sub>8</sub>.



**Figure S20** <sup>13</sup>C{<sup>1</sup>H} NMR spectrum (+25 °C, 126 MHz, THF-d<sub>8</sub>) of [EtAl(6-Me-2py)<sub>3</sub>YbI(thf)<sub>2</sub>] (**5**). The signals of THF (insert) appear partially overlapped with the signals of THF-d<sub>8</sub>.

Note: The C(6)-CH<sub>3</sub> signal at 25.42 ppm overlapped with the THF-d<sub>8</sub> signal, but was detected through a <sup>1</sup>H-<sup>13</sup>C HMQC experiment (see Fig S22).

— 129.5443

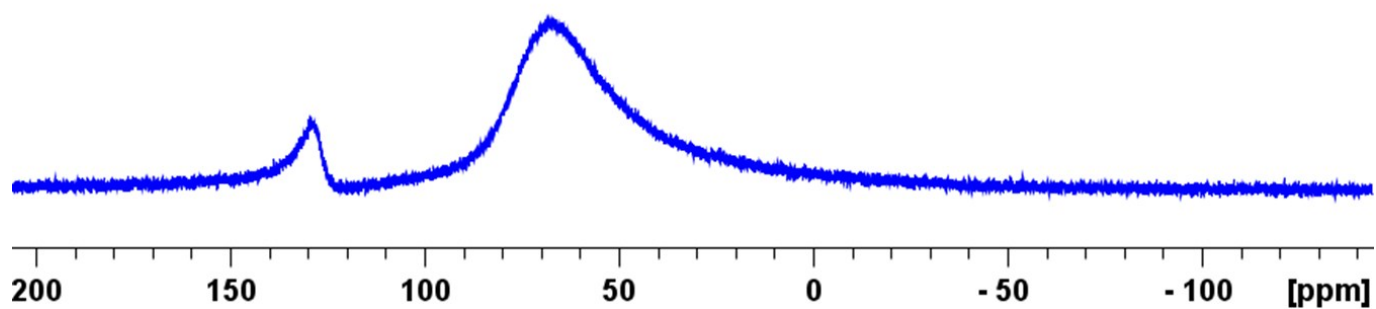
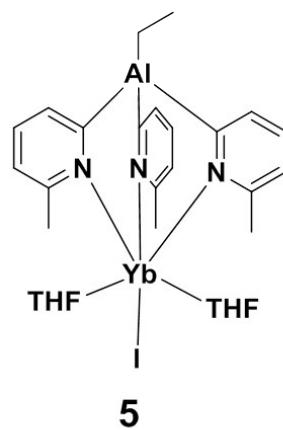


**Figure S21**  $^{27}\text{Al}$  NMR spectrum (+25 °C, 130 MHz,  $\text{THF-d}_8$ ) of  $[\text{EtAl}(\text{6-Me-2py})_3\text{YbI}(\text{thf})_2]$  (**5**).

Note: The broad signal at around 65ppm in the  $^{27}\text{Al}$  NMR spectrum arises from the probe background.

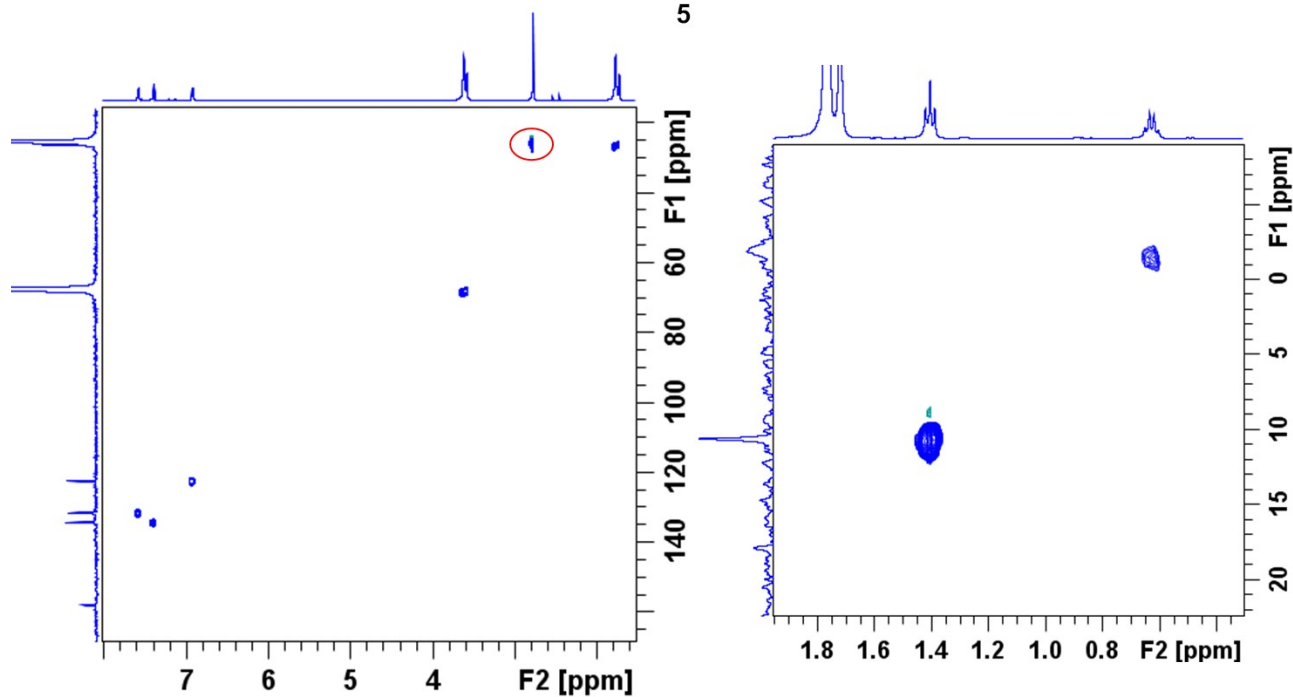
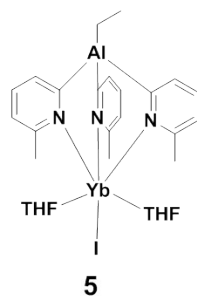


**Figure S22** Selected regions of the  $^1\text{H}$ - $^{13}\text{C}$  HMQC NMR spectrum (+25 °C, 500 MHz,  $\text{thf-d}_8$ ) of  $[\text{EtAl}(\text{6-Me-2py})_3\text{YbI}(\text{thf})_2]$  (**5**). Left, a selected region showing that the C(6)- $\text{CH}_3$  signal at 25.42 ppm overlaps with the  $\text{thf-d}_8$  signal, which is marked with a red circle. Right, the ethyl region, showing that the broad Al- $\text{CH}_2$  carbon resonance can be detected and definitively assigned. Note: The 1D  $^{13}\text{C}\{^1\text{H}\}$  NMR spectrum processed with a line broadening (lb) of 20 Hz is shown as the 'external projection'.

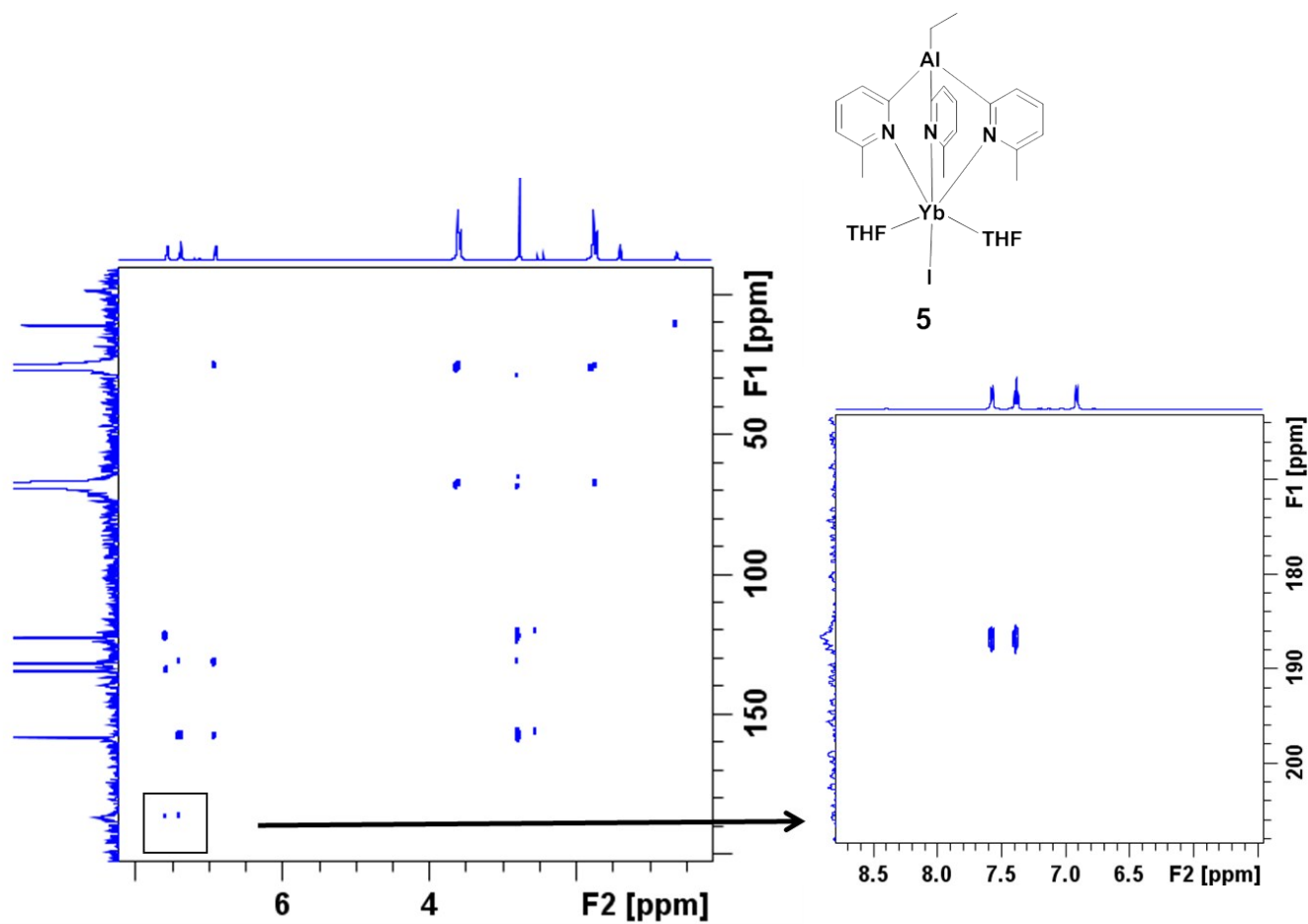


**Figure S23** Selected regions of the  $^1\text{H}$ - $^{13}\text{C}$  HMBC NMR spectrum (+25 °C, 500 MHz,  $\text{THF-d}_8$ ) of  $[\text{EtAl}(\text{6-Me-2py})_3\text{Yb}(\text{thf})_2]$  (**5**). The expansion shows that the broad Al-C(2) signal can be easily detected in the  $^1\text{H}$ - $^{13}\text{C}$  HMBC NMR spectrum. Note: The 1D  $^{13}\text{C}\{^1\text{H}\}$  NMR spectrum processed with a line broadening (lb) of 20Hz is shown as the 'external projection'.

# NMR spectra for compound 7, [EtAl(6-Br-2-py)<sub>3</sub>]<sub>2</sub>Yb

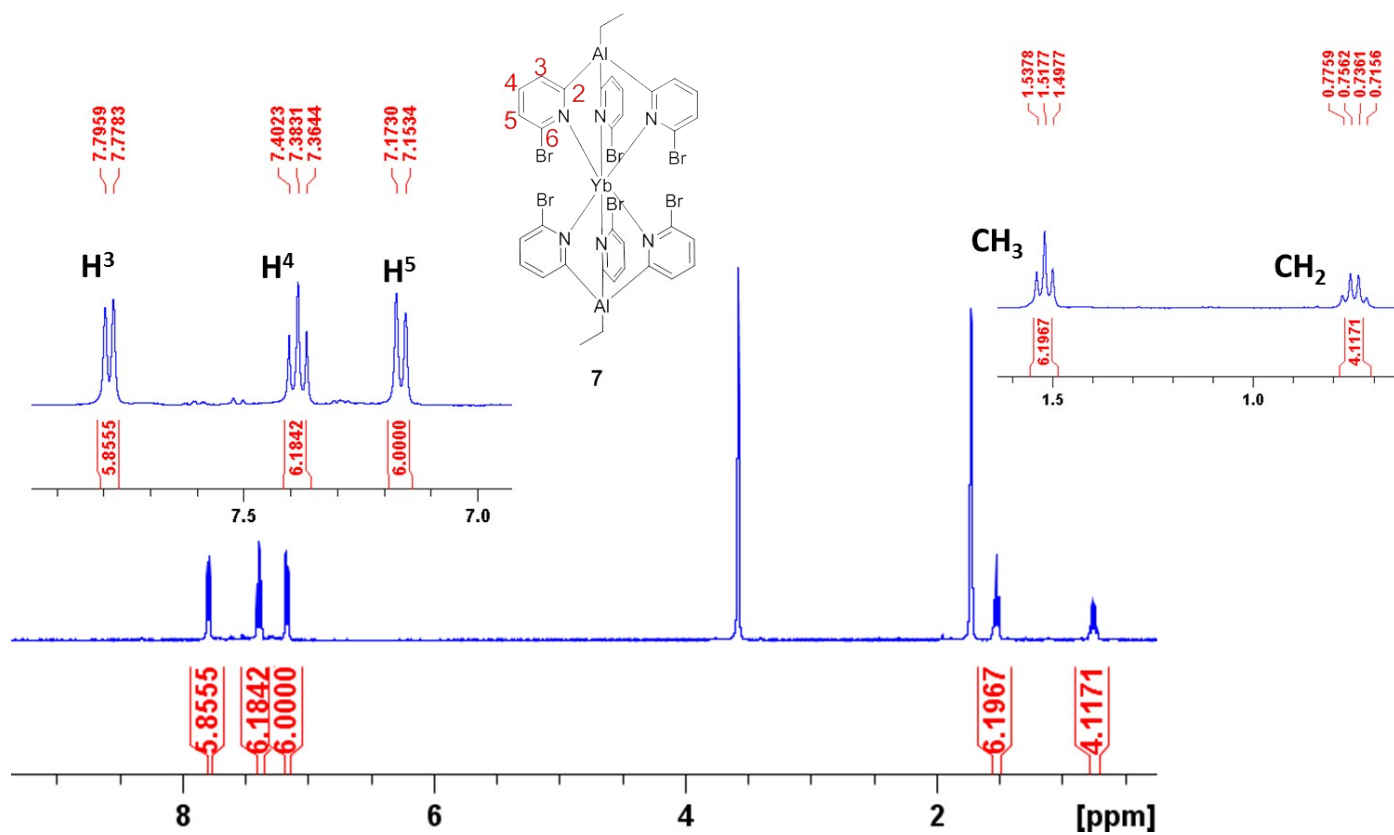
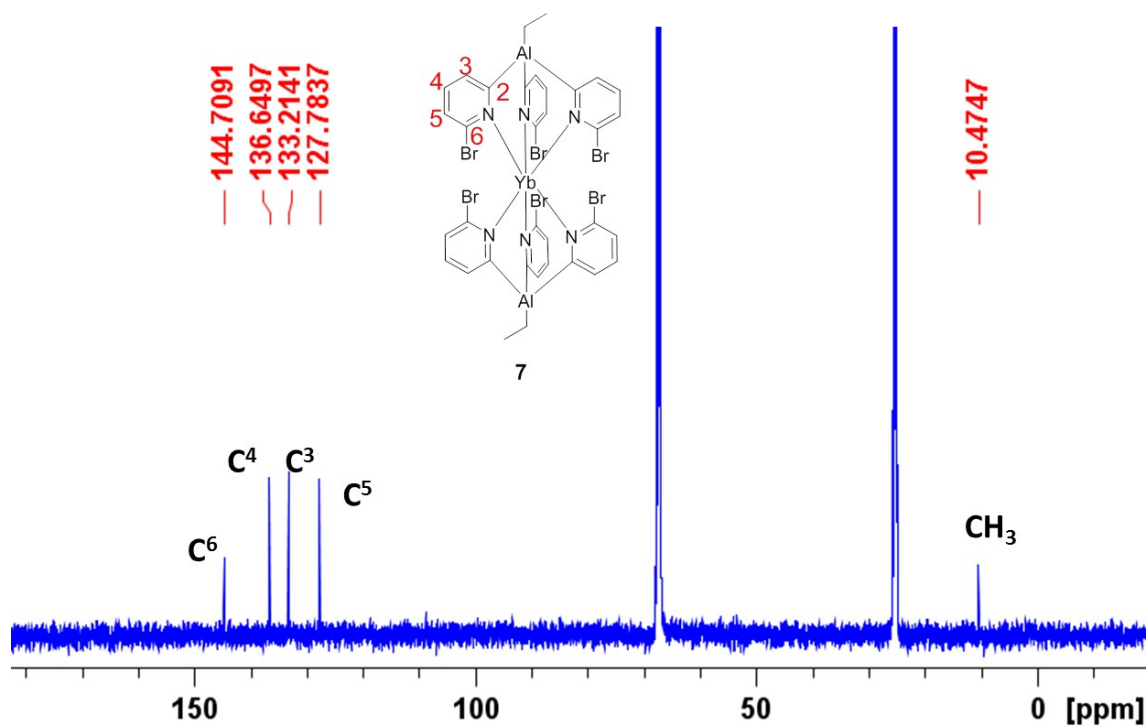
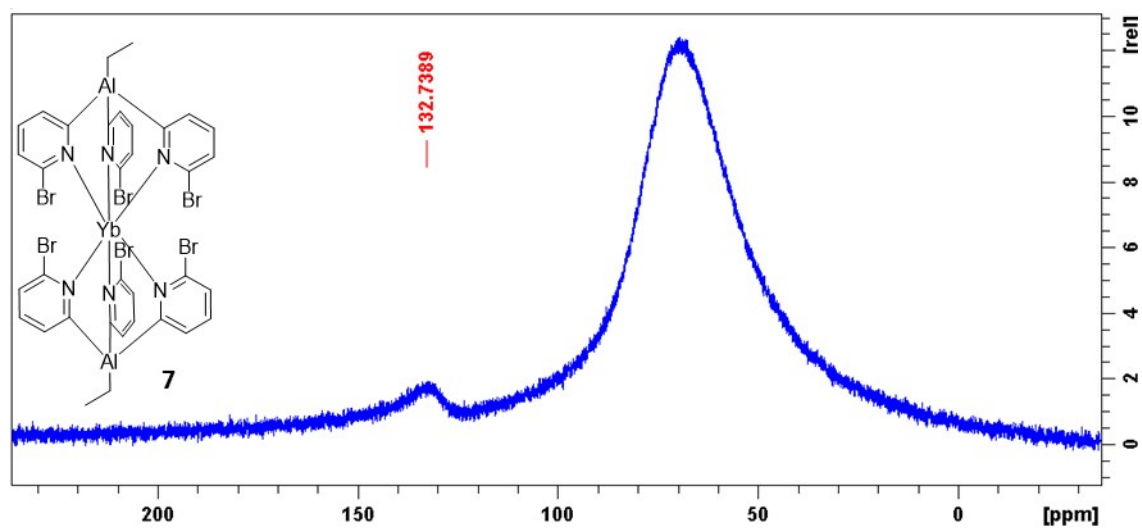


Figure S24 <sup>1</sup>H NMR spectrum (+25 °C, 400 MHz, thf-d<sub>8</sub>) of [EtAl(6-Br-2-py)<sub>3</sub>]<sub>2</sub>Yb (7).



**Figure S25**  $^{13}\text{C}\{^1\text{H}\}$  NMR spectrum ( $+25\text{ }^\circ\text{C}$ , 126 MHz,  $\text{thf-d}_8$ ) of  $[\text{EtAl}(\text{6-Br-2-py})_3]_2\text{Yb}$  (**7**). Direct observation of the Al-bonded C atoms was not possible in the  $^{13}\text{C}\{^1\text{H}\}$  spectrum due to their low-intensity broad resonances and the low solubility of **7**. However, their detection was possible through  $^1\text{H}$ - $^{13}\text{C}$  HMQC and  $^1\text{H}$ - $^{13}\text{C}$  HMBC NMR experiments (see Fig S28 and S29).



**Figure S26**  $^{27}\text{Al}$  NMR spectrum (+25 °C, 130 MHz,  $\text{thf-d}_8$ ) of  $[\text{EtAl}(\text{6-Br-2-py})_3]_2\text{Yb}$  (**7**).

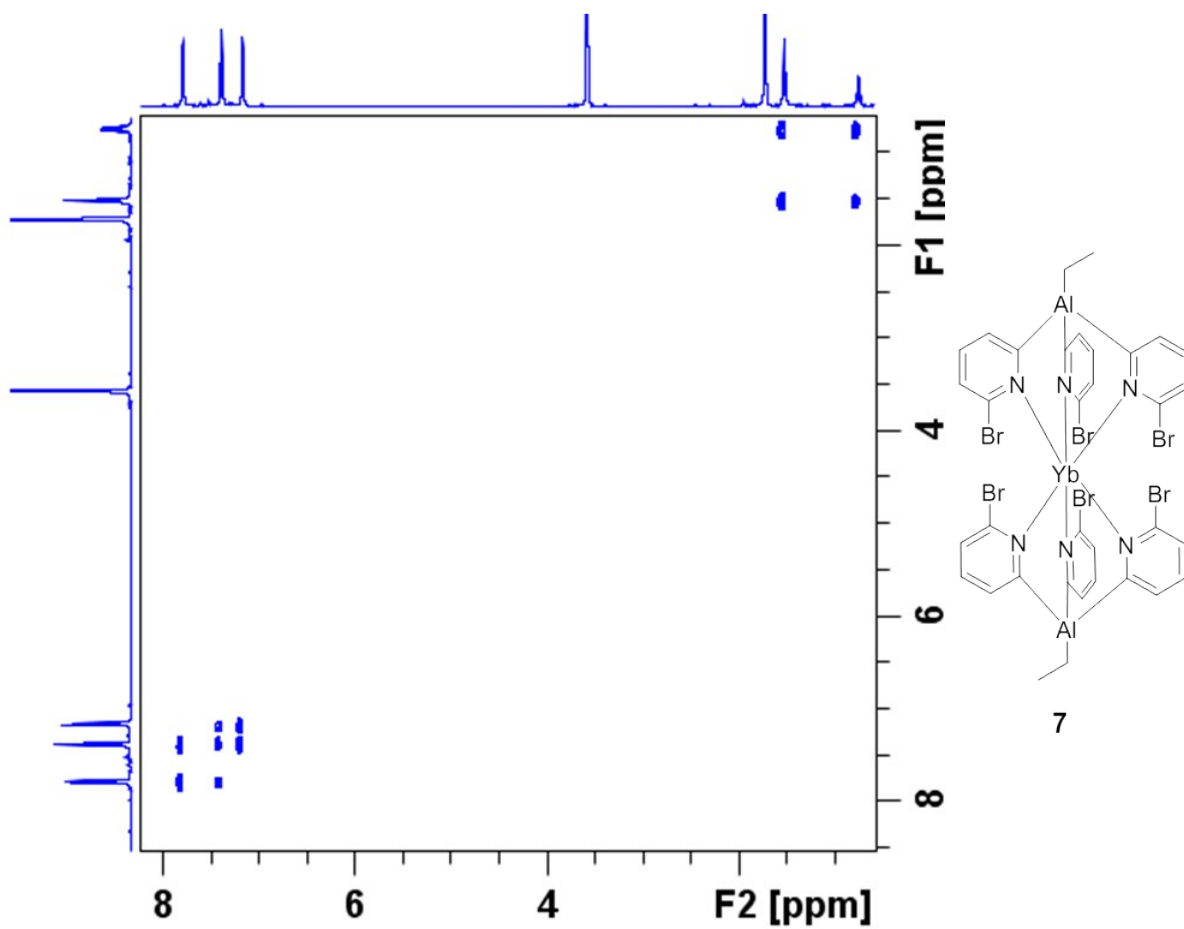
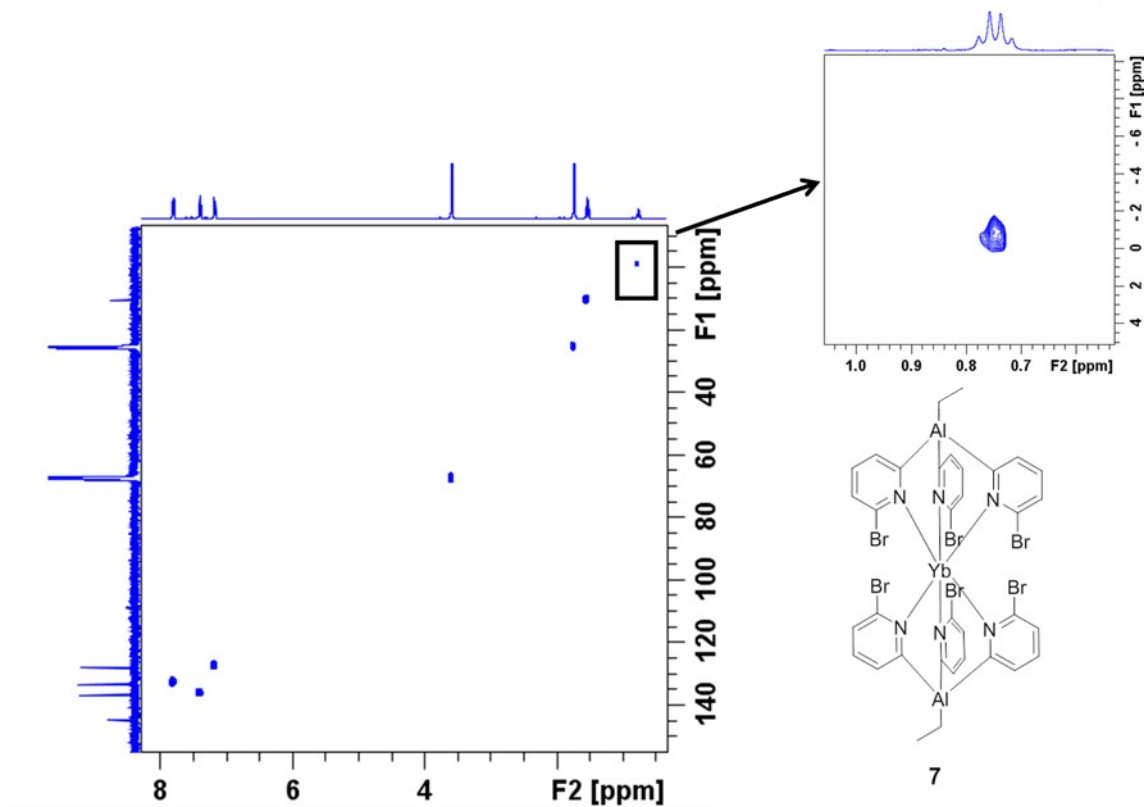
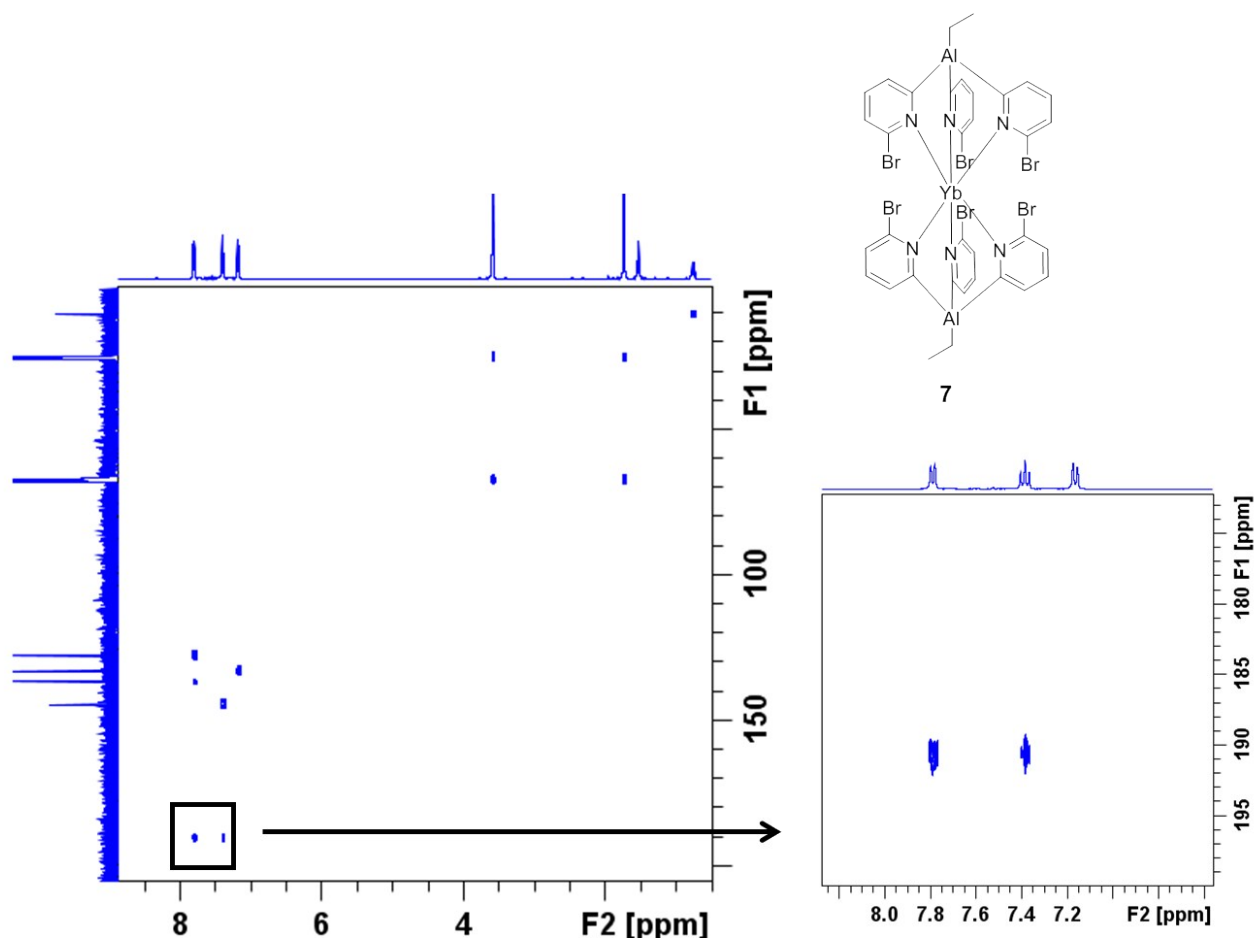


Figure S27  $^1\text{H}$ - $^1\text{H}$  COSY NMR spectrum (+25 °C, 500 MHz,  $\text{thf-d}_8$ ) of  $[\text{EtAl}(\text{6-Br-2-py})_3]_2\text{Yb}$  (7).



**Figure S28**  $^1\text{H}$ - $^{13}\text{C}$  HMQC NMR spectrum (+25 °C, 500 MHz,  $\text{thf-d}_8$ ) of  $[\text{EtAl}(\text{6-Br-2-py})_3]_2\text{Yb}$  (**7**). Direct observation of the Al-bonded C atoms was not possible in the  $^{13}\text{C}\{^1\text{H}\}$  spectrum due to their low-intensity broad resonances and the low solubility of **7**. However, the broad  $^{13}\text{C}$  signal for Al- $\text{CH}_2$  was detected in the  $^1\text{H}$ - $^{13}\text{C}$  HMQC NMR spectrum (insert).



**Figure S29**  $^1\text{H}$ - $^{13}\text{C}$  HMBC NMR spectrum (+25 °C, 500 MHz,  $\text{THF-d}_8$ ) of  $[\text{EtAl}(\text{6-Br-2-py})_3]_2\text{Yb}$  (**7**). Direct observation of Al-bonded C atoms was not possible in the  $^{13}\text{C}\{^1\text{H}\}$  spectrum due to their low-intensity broad resonances and low solubility of **7**. However, the broad  $^{13}\text{C}$  signal for Al-C2 was detected in the  $^1\text{H}$ - $^{13}\text{C}$  HMBC NMR spectrum (insert).

## X-ray crystal structures of compounds

### X-ray Crystallographic Studies

Data were collected using Bruker Apex,2 Bruker APEX3 or GIS, processed using SAINT and SADABS. Structures were solved using SHELXT (Sheldrick, 2015) and refined using SHELXL (Sheldrick, 2015).

**Table S1** Details of the data collection and refinement of compounds **1–6**·THF

Compound	<b>3</b> ·Lil	<b>4</b> ·Lil	<b>3</b>	<b>4</b>	<b>5</b> ·thf	<b>6</b> ·2thf
chemical formula	C <sub>56</sub> H <sub>62</sub> Al <sub>2</sub> EuLi <sub>2</sub> N <sub>6</sub> O <sub>4</sub>	C <sub>64</sub> H <sub>94</sub> Al <sub>2</sub> Li <sub>2</sub> N <sub>6</sub> O <sub>6</sub> Yb	C <sub>40</sub> H <sub>46</sub> Al <sub>2</sub> EuN <sub>6</sub>	C <sub>40</sub> H <sub>46</sub> Al <sub>2</sub> N <sub>6</sub> Yb	C <sub>28</sub> H <sub>39</sub> AlIn <sub>3</sub> O <sub>2</sub> Yb·thf	C <sub>34</sub> H <sub>28</sub> Al <sub>2</sub> Br <sub>6</sub> EuN <sub>6</sub> ·2thf
<i>FW</i>	1372.85	1538.13	816.75	837.83	848.64	1350.21
crystal system	triclinic	triclinic	tetragonal	monoclinic	monoclinic	Triclinic
space group	<i>P</i> -1	<i>P</i> -1	<i>P</i> 4 <sub>3</sub> 2 <sub>1</sub> 2	<i>P</i> 2 <sub>1</sub> / <i>n</i>	<i>P</i> 2 <sub>1</sub> / <i>m</i>	<i>P</i> -1
<i>a</i> (Å)	9.4740(2)	9.6229(3)	10.5238(2)	11.732(2)	10.9332(3)	10.8508(2)
<i>b</i> (Å)	10.4528(2)	10.7281(4)	10.5238(2)	19.517(3)	14.2445(5)	10.9222(2)
<i>c</i> (Å)	17.1753(4)	17.8161(6)	35.4237(7)	16.296(3)	11.6132(4)	11.6496(3)
$\alpha$ (°)	98.918(1)	97.034(2)	90	90	90	92.214(1)
$\beta$ (°)	102.051(1)	105.055(2)	90	96.376(6)	105.9277(4)	113.358(1)
$\gamma$ (°)	108.705(1)	97.684(2)	90	90	90	108.481(1)
<i>V</i> (Å <sup>3</sup> )	1529.62(6)	1736.27(10)	3923.19(17)	3708.2(11)	1739.18(10)	1180.53(4)
<i>Z</i>	1	1	4	4	2	1
Radiation	MoK $\alpha$	CuK $\alpha$	CuK $\alpha$	MoK $\alpha$	CuK $\alpha$	MoK $\alpha$
<i>T</i> (K)	220(2)	180(2)	180(2)	199(2)	180(2)	180(2)
$\rho_{\text{calc}}$ (g/cm <sup>3</sup> )	1.490	1.471	1.383	1.501	1.621	1.899
$\mu$ (mm <sup>-1</sup> )	2.109	10.110	12.144	2.607	12.449	6.484
reflections collected ( <i>R</i> <sub>int</sub> )	16615 (0.038)	23992 (0.045)	21577 (0.088)	22486 (0.133)	21396 (0.079)	12740 (0.049)
independent reflections	6772	5808	3464	6409	3205	5257
<i>R</i> <sub>1</sub> [ <i>I</i> > 2 $\sigma$ ( <i>I</i> )]	0.0377	0.0431	0.0405	0.0652	0.0497	0.0459
<i>wR</i> <sub>2</sub> (all data)	0.0828	0.1045	0.0756	0.1585	0.1400	0.1421
Goodness of fit, <i>S</i>	1.050	1.013	1.010	1.000	1.081	0.949
Flack parameter			-0.012(4)			
CCDC number	1587534	1587538	1587533	1587535	1587537	1587536

**Table S2** Comparison of selected bond lengths (Å) and angles (°) for the 2-py ligands

Compound	<b>3</b> ·Lil	<b>4</b> ·Lil	<b>3</b>	<b>4</b>	<b>5</b> ·thf	<b>6</b> ·2thf
C <sub>Et</sub> -Al	1.988(4)	1.994(5)	1.996(6)	1.96(1)-1.97(1)	1.98(1)	1.994(5)
C <sub>py</sub> -Al	2.014(4)-2.036(4)	2.007(5)-2.023(5)	2.010(6)-2.025(7)	1.96(1)-2.02(1)	2.022(7)-2.035(5)	2.010(5)-2.019(6)
Al...Ln	3.564(1)	3.459(1)	3.565(2)	3.431(3)-3.444(3)	3.448(3)	3.807(6)
N <sub>1</sub> -Ln	2.693(3)	2.564(4)	2.713(6)	2.542(8)-2.546(7)	2.505(8)	2.795(4)
N <sub>2</sub> -Ln	2.696(3)	2.611(4)	2.674(5)	2.560(8)-2.587(9)	2.534(5)	2.756(4)
N <sub>3</sub> -Ln	2.689(3)	2.575(4)	2.655(6)	2.585(8)-2.585(9)	2.534(5)	2.754(4)
C <sub>py</sub> -Al-C <sub>py</sub>	104.6(2)-113.4(1)	105.6(2)-112.4(2)	101.6(2)-112.1(3)	101.6(2)-112.1(3)	104.3(4)-108.7(2)	105.8(2)-111.5(3)
Al-C <sub>py</sub> -N	121.4(4)-123.8(3)	120.3(2)-123.9(3)	119.7(5)-123.8(4)	121.7(7)-124.7(7)	119.1(6)-121.7(5)	120.3(4)-124.0(4)
N-Ln-N	88.5 (1)-91.51(9)	85.6(1)-94.4(1)	85.4(2)-91.1(2)	84.7(3)-94.7(3)	82.0(3)-98.7(2)	84.1(1)-95.9(1)

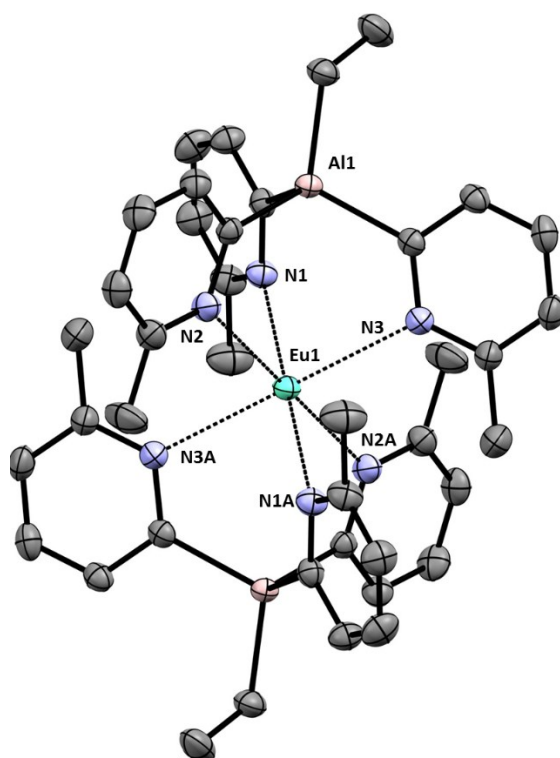


Figure S30 X-ray crystal structure of  $[\text{EtAl}(\text{6-Me-2-py})_3]_2\text{Eu}$  (**3**). H-atoms have been omitted for clarity.

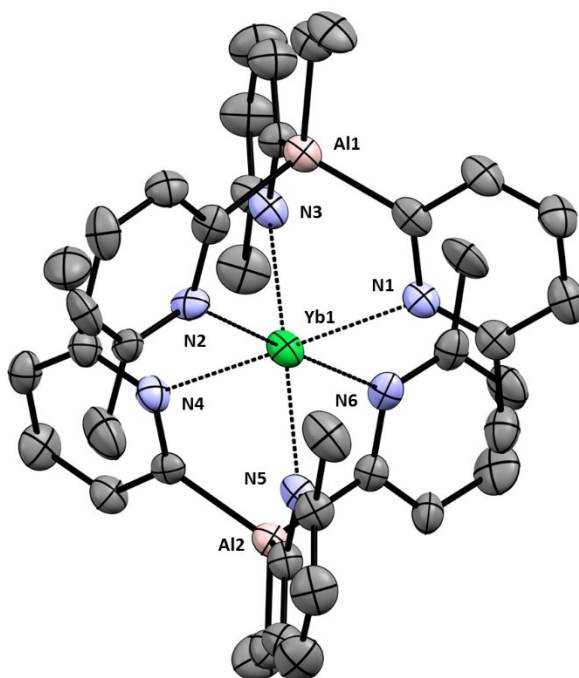
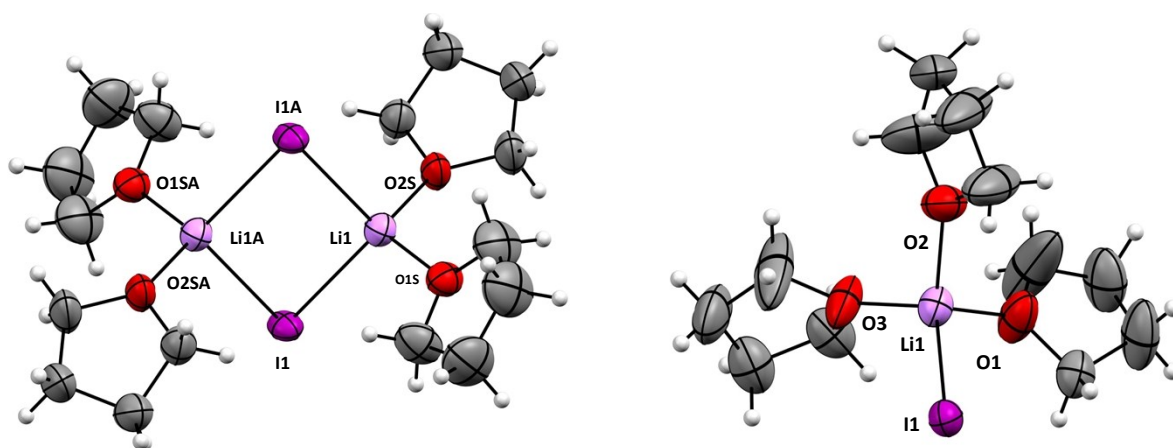


Figure S31 X-ray crystal structure of  $[\text{EtAl}(\text{6-Me-2-py})_3]_2\text{Yb}$  (**4**). H-atoms have been omitted for clarity.



**Figure S32** (left) the  $[\text{thf}_2\text{Li}(\mu\text{-I})]_2$  dimer units of  $3 \cdot \text{LiI}$ ; (right) the  $(\text{thf})_3\text{LiI}$  units of  $4 \cdot \text{LiI}$ .